Université d'Ottawa • University of Ottawa

PERMISSION DE REPRODUIRE ET DE DISTRIBUER LA THÈSE

PERMISSION TO REPRODUCE AND DISTRIBUTE THE THESIS

NOM DE L'AUTEUR / NAME OF AUTHOR:	FALLER, Elliott
ADRESSE POSTALE / MAILING ADDRESS:	11-167 RUSSEL AVENUE OTTAWA ON K1N7X3
GRADE / DEGREE:	**ANNÉE D'OBTENTION / YEAR GRANTED**
M.Sc. (Biology)	2003
TITRE DE LA THÈSE / TITLE OF THESIS: MODULATION DE MICROTUBULE DYNAMICS BY THE MICROTUBULE-ASSOCIATED PROTEIN MAPLA	

L'auteur permet, par la présente, la consultation et le prêt de cette thèse en conformité avec les règlements établis par le bibliothécaire en chef de l'Université d'Ottawa. L'auteur autorise aussi l'Université d'Ottawa, ses successeurs et cessionnaires, à reproduire cet exemplaire par photographie ou photocopie pour fins de prêt ou de vente au prix coûtant aux bibliothèques ou aux chercheurs qui en feront la demande.

Les droits de publication par tout autre moyen et pour vente au public demeureront la propriété de l'auteur de la thèse sous réserve des règlements de l'Université d'Ottawa en matière de publication de thèses.

The author hereby permits the consultation and the lending of this thesis pursuant to the regulations established by the Chief Librarian of the University of Ottawa. The author also authorizes the University of Ottawa, its successors and assignees, to make reproductions of this copy by photographic means or by photocopying and to lend or sell such reproductions at cost to libraries and to scholars requesting them.

The right to publish the thesis by other means and to sell it to the public is reserved to the author, subject to the regulations of the University of Ottawa governing the publication of theses.

N.B. LE MASCULIN COMPREND ÉGALEMENT LE FÉMININ

April 28 · 2003

DATE

(AUTEUR) SIGNATURE (AUTHOR)

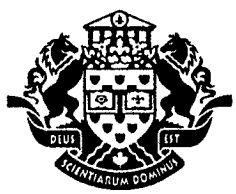

Université d'Ottawa · University of Ottawa

Université d'Ottawa · University of Ottawa

FACULTÉ DES ÉTUDES SUPÉRIEURES ET POSTDOCTORALES

FACULTY OF GRADUATE AND POSTDOCTORAL STUDIES

FALLER, Elliott M.

AUTEUR DE LA THÈSE - AUTHOR OF THESIS

M.Sc. (Biology)

GRADE - DEGREE

Biology

FACULTÉ, ÉCOLE, DÉPARTEMENT - FACULTY, SCHOOL, DEPARTMENT

TITRE DE LA THÈSE - TITLE OF THE THESIS

Modulation of Microtubule Dynamics by the Microtubule-Associated Protein MAP1a

David L. Brown

DIRECTEUR DE LA THÈSE - THESIS SUPERVISOR

EXAMINATEURS DE LA THÈSE - THESIS EXAMINERS

C. Martin

L. Sabourin

J. Cheetham

J.-M. De Koninck, Ph.D.

LE DOYEN DE LA FACULTÉ DES ÉTUDES SUPÉRIEURES ET POSTDOCTORALES

SIGNATURE

DEAN OF THE FACULTY OF GRADUATE AND POSTDOCTORAL STUDIES

Modulation of Microtubule Dynamics by the Microtubule-Associated Protein MAP1a

By

Elliott M. Faller

A thesis submitted to the Faculty of Graduate and Postdoctoral Studies, University of Ottawa, in partial fulfillment of the requirements for the degree of Master of Science, Ottawa-Carleton Institute of Biology

January, 2003

I hereby declare that I am the sole author of this thesis.

I authorize the University of Ottawa to lend this thesis to other institutions or individuals for the purpose of scholarly research.

I further authorize the University of Ottawa to reproduce this thesis by photocopying or by other means, in total or part, at the request of other institutions or individual for the purpose of scholarly research.

Elliott M. Faller

ACKNOWLEDGEMENTS

I would like to thank Dr David L. Brown for providing me with the opportunity to work with him on this project. In addition to the helpful suggestions and guidance he provided, I would specially like to thank him for his supervision of my writing.

I would like to thank the members of my committee Dr. Jim Cheetham and Dr. Luc Sabourin for their advice and suggestions during the course of my thesis research.

I would also like to thank my labmates Tania Villeneuve and Nicole Ungureanu. You welcomed me into the lab helped me make a smooth transition from microbiology to cell biology.

I thank Andrew Ochalski for his hours and days of assistance to develop the microscopy techniques I used in the present study.

In closing I would like to thank my wife Laura for her love and support during the course of my thesis research.

TABLE OF CONTENTS

ABBREVIATIONS

AA	amino acid
MEM	Eagle's minimal essential media
BSA	bovine serum albumin
CCD	charge-cooled device
cDNA	complementary deoxyribonucleic acid
cs	coverslip
CY3	indocarbocyanine
ddH_2O	double distilled, deionized water
DMSO	dimethyl sulfoxide
DNA	deoxyribonucleic acid
DTT	dithiothreitol
EC	embryonal carcinoma
ECL	enhanced chemiluminescence
EDTA	ethylenediaminetetraacetic acid disodium salt
EGTA	ethyene glycol bis (β-aminoethylether)
FCS	fetal calf serum
GTP	guanidine triphosphate
HMW	high molecular weight
HRP	horse radish peroxidase

kb	kilobase
kDA	kilodalton
LB	Luria Bertani
LC	light chain
mAb	monoclonal antibody
MAP	microtubule-associated protein
mRNA	messenger ribonucleic acid
MES	N-morpholinoethanesulfonic acid
MTOC	microtubule organizing center
MW	molecular weight
NC	nitrocellulose
pAb	polyclonal antibody
PBS	phosphate buffered saline
PC	phosphocellulose
PEFA	p-aminoethylbenzenesulfonyl fluoride
PEM	PIPES/EGTA/$MgCl_2$ buffer
PIPES	piperazine-N.N'-bis-2-ethanesulfonic acid
RT	room temperature
SDS-PAGE	sodium dodecyl sulfate polyacrylamide gel electrophoresis

LIST OF FIGURES

ABSTRACT

Structural microtubule-associated proteins (MAPs) are capable of interacting with tubulin dimers to regulate the various dynamic stages of microtubules. MAP1a is predominant in the neuronal cell body, axons and dendrites of mature neurons. MAP1a has been shown to bind microtubules to promote microtubule assembly *in vitro*. The MAP1a heavy chain molecule is associated with three light chains. The heavy chain, and all three light chains appear to associate with microtubules independent of each other. The purpose of this project was to measure the impact of myc-tagged MAP1a fragments and myc-tagged light chains associated with MAP1a on microtubule dynamic phases *in vivo*. Cells from an epithelial kidney cell line (LLCPK1) that had been permanently transfected with human GFP-α tubulin were transiently transfected with myc tagged MAP1a heavy and light chain fragments. Cells expressing MAP1a and light chain fragments were used to make direct observations of microtubule dynamics in living cells using fluorescence microscopy. Microtubule ends were photographed at 4-second intervals using a digital camera over a 2-minute duration. All truncated MAP1a heavy chain fragments that contained the microtubule-binding domain were shown to associate with microtubules. MAP1a fragments containing portions of the projection domain promoted growth and stability of microtubules. Truncated fragments containing different regions of the projection domain of MAP1a demonstrated variations in their impact on microtubule dynamic events by promoting growth or inhibition of shortening phases. Similar to full length MAP1a, LC3 also appeared to promote microtubule

growth and stability. Results from the present study suggest that MAP1a and LC3 promote slow, stable growth of microtubules. This type of growth may be important in the maintenance and restructuring of adult neurons.

RESUME

Les protéines associées aux microtubules (MAPs) structuraux sont capables d'interagir avec la tubuline pour régulariser les différentes phases dynamiques des microtubules. MAP1a est prédominante dans le corps des neuronnes ainsi que dans les axones et les dendrites des neuronnes matures. MAP1a aide à l'assemblage des microtubules *in vitro.* La chaîne lourde et les 3 chaînes légères peuvent se liées aux microtubules d'une façon autonome. Le but de ce projet est de mesurer l'impacte de différentes sections de la chaîne lourde de MAP1a, étiquetées avec 6myc, sur les phases dynamiques des microtubules *in vivo.* On utilise des cellules de reins épithéliales (LLCPK1), transfectées d'une façon permanentes avec la α-tubuline-GFP, exprimant les chaînes lourdes et légères de MAP1a grâce à la transfection transiente. La microscopie fluorescente et ces cellules ont été utilisées pour faire des observations sur la dynamique des microtubules dans des cellules vivantes. Le bout des microtubules ont été photographiés à des intervalles de 4 secondes grâce à une caméra digitale sur une période de 2 minutes. Tous les sections de la chaîne lourde de MAP1a qui contenait la partie importante pour les interactions MAP1a-microtubules se sont liées aux microtubules. Seulement les sections de la chaîne lourde de MAP1a qui contenait des portions du domaine projectif ont été capable de promouvoir la croissance et la stabilité des microtubules. Ces différentes sections ont eu un impacte variable sur la dynamique des microtubules soit en augmantant la croissance ou en inhibant le raccourcissement. Pareil comme la chaîne lourde complète de MAP1a, LC3 favorise la croissance

lente et constante des microtubules. Ce type de croissance peut être importante dans la soutenance et la restructuration des neuronnes adultes.

I. INTRODUCTION

Microtubules are important eukaryotic cell structures involved in many roles such as determining cell shape, polarity, mitosis, motility and intracellular transport (Avila et al., 1994). Microtubules are composed of alpha (56 kDa) and beta tubulin (54 kDa) heterodimers. Tubulin dimers associate end to end to form protofilaments (Mandelkow and Mandelkow, 1995). Typically, 13 protofilaments associate laterally to form a hollow tubular structure of approximately 25 nm in diameter (Laferriere et al., 1997 for review) (see figure 1). Microtubules nucleate at, and elongate from, the centrosome (see figure 2). Microtubules elongate to the periphery of the cell according to the inherent dynamic instability properties of microtubules (Mitchison and Kischner, 1984). Two populations of microtubules appear to exist in interphase cells; a stable population of microtubules that remain in an attenuated state, and dynamic population that goes through periods of growth and shortening (Mitchison and Kirschner, 1984; Schulze and Kirschner, 1986)

A. Microtubule Dynamics

Individual microtubules exist in phases of elongation and shortening, by addition or loss of tubulin subunits (see figure 3), with infrequent and abrupt changes between these phases referred to as catastrophe (elongation to shortening transition), rescue (shortening to elongation transition), and pause (Cassimeris, 1993). The dynamic instability model of microtubule growth suggests that microtubules are inherently

Figure 1: Schematic representation of the arrangement of protofilaments and α/β-tubulin dimers and in a microtubule (Reproduced from Valliant 1997).

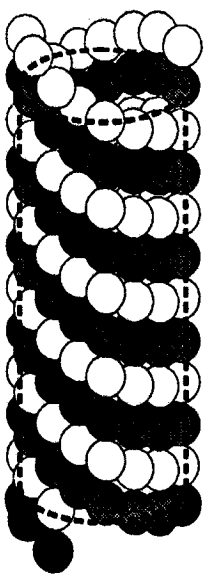

SIDE VIEW OF A MICROTUBULE

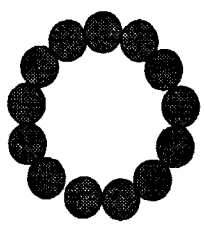

CROSS SECTION OF A MICROTUBULE

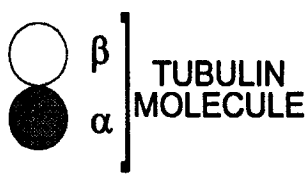

Figure 2: Schematic representation of: A) interphase microtubule organization and B) the addition of α/β-tubulin dimers to the + end of microtubules radiating from the Microtubule Organizing Centre (MTOC) (Reproduced from Valliant 1997).

A

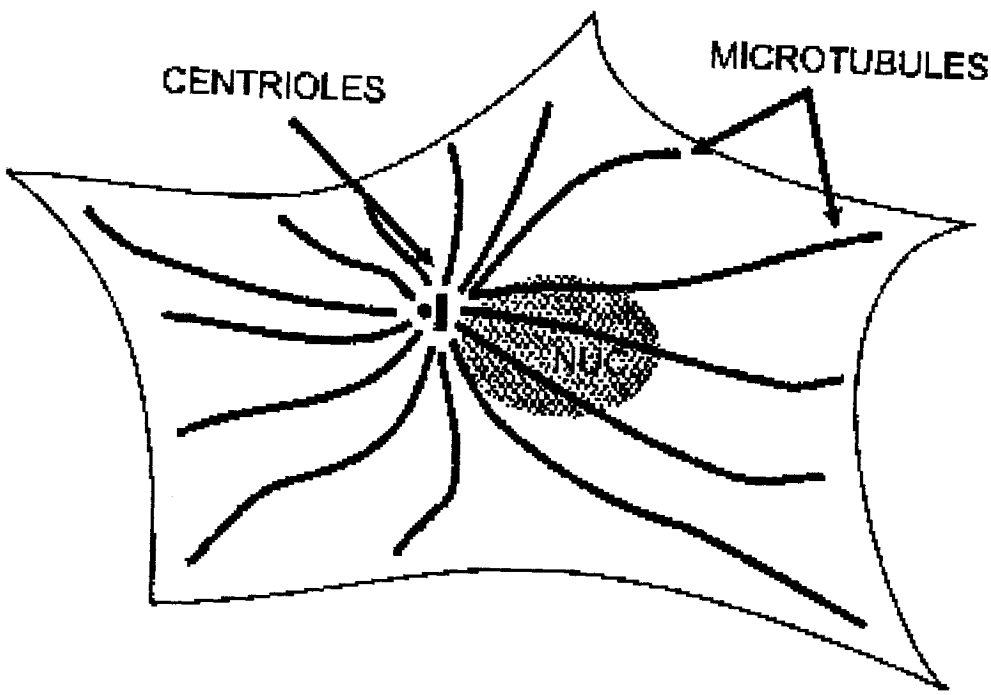

B

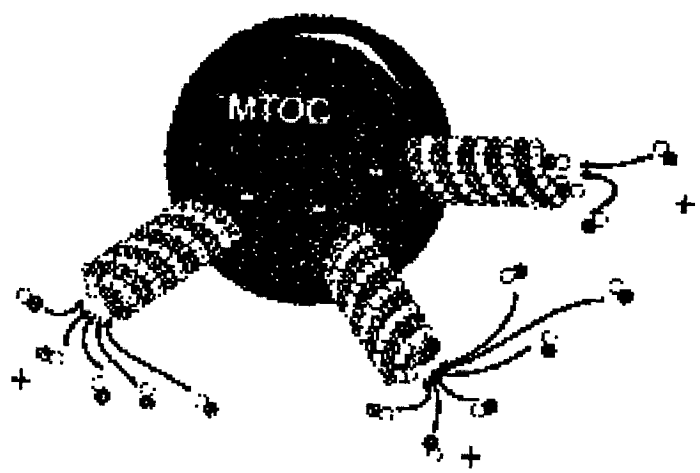

Figure 3: A schematic representation of the 3 dynamic phases of microtubules: growth (caused by addition α/β-tubulin dimers to microtubule ends), shortening (caused by a loss of α/β-tubulin dimers from microtubule ends) and pause (no change in the net length of microtubules) (from Kirschner and Mitchison, 1986).

Pause

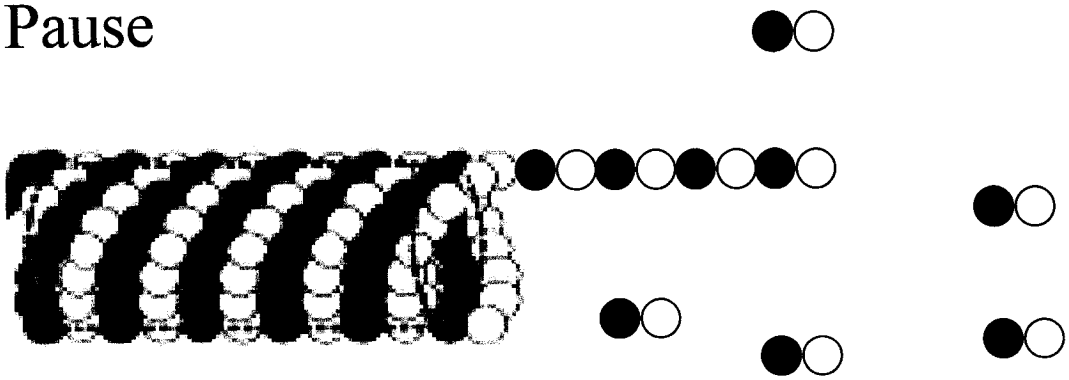

Growth

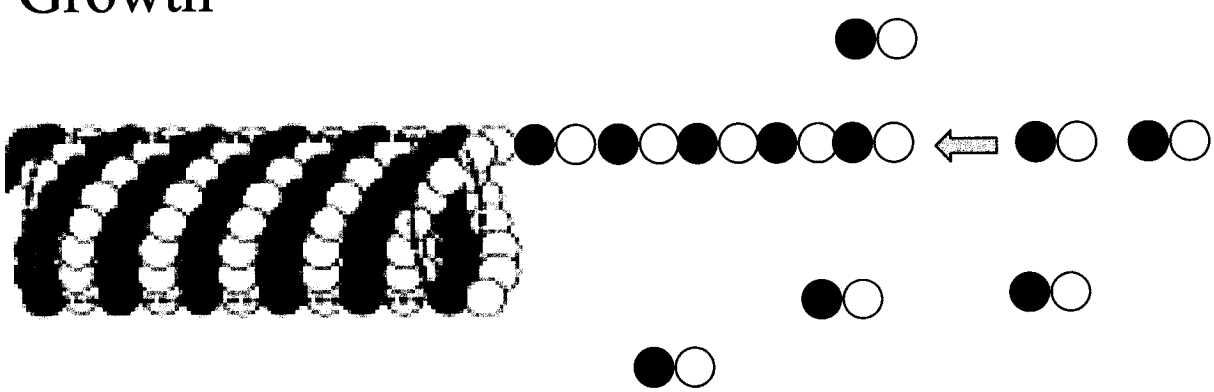

Shortening

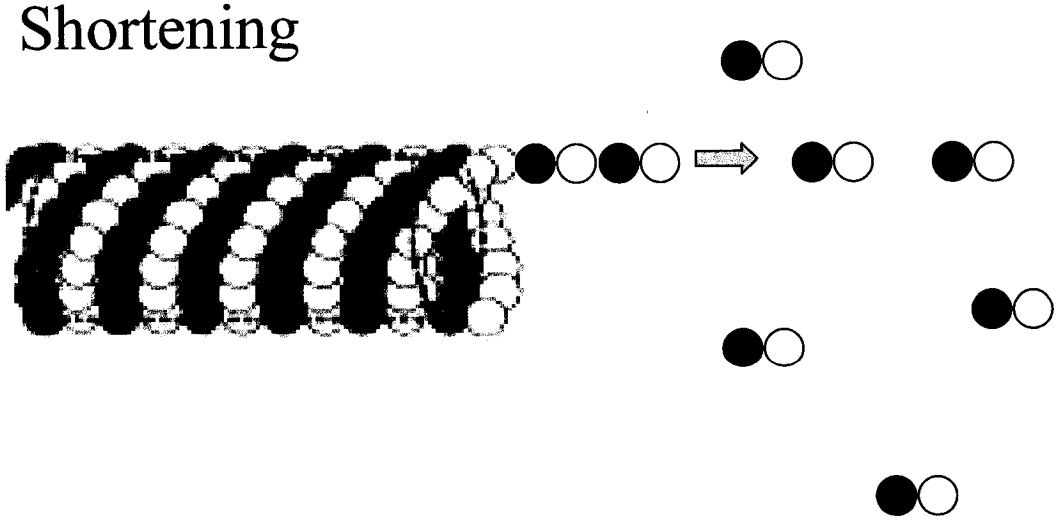

unstable. *In vitro* microtubule rates of elongation are slower than rates measured *in vivo* and display greater instability as a result of increased phase transitions (Cassimeris et al., 1988). Interphase elongation rates are typically 4-7 μm/min and shortening rates are 10-20 μm/min. The levels of soluble tubulin present in the cytoplasm surrounding microtubules determine lengthening and shortening of microtubules. The rate of microtubule elongation has been found to be directly proportional to the concentration of tubulin, with higher tubulin concentrations corresponding to increased assembly rates (Mitchison and Kirschner, 1984). Free tubulin dimers that bind GTP are incorporated onto the growing microtubule end (see figure 4). Once incorporated, GTP is hydrolyzed to GDP. This forms a cap at the distal end of a microtubule composed of tubulin dimers with GTP at their β-tubulin exchangeable sites. The stable GTP cap protects a labile core of tubulin-GDP from depolymerization. Presence of the GTP cap encourages elongation, while loss of the cap induces shortening events (Mitchison and Kirschner, 1984). Different cell types display differences in growth, shortening and attenuation of microtubules *in vivo* (Shelden and Wadsworth, 1993). Changes in phosphorylation levels of tubulin have also been shown to alter dynamic instability characteristics of microtubules *in vitro* and *in vivo* (Verde et al., 1990; Lieuvin et al., 1994).

B. Heterogeneity of Tubulin

Several different tubulin isotypes are expressed in vertebrate cells (Field et al., 1984). Brain tissue expresses the largest variety (5 α, 5 β) of tubulin isotypes (Sullivan

Figure 4: A model for the regulation of microtubule dynamics by GTP hydrolysis.

(as proposed by Kirschner and Mitchison, 1986).

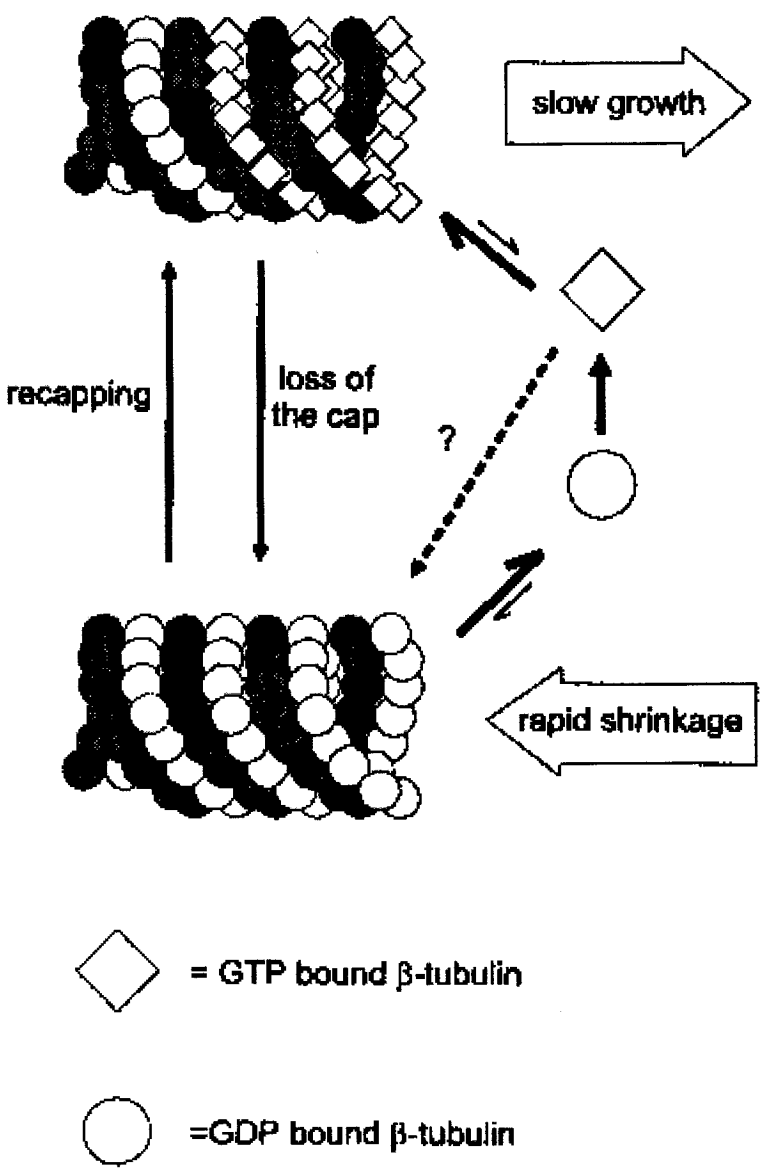
slow growth
recapping
loss of
the cap
?
rapid shrinkage
= GTP bound β-tubulin
=GDP bound β-tubulin

and Cleveland, 1986; Villasante et al., 1986; Joshi and Cleveland, 1989). Tubulin isotypes vary in their carboxy terminus 15 amino acid end sequences (Sullivan and Cleveland 1986). Developmentally regulated expression of tubulin isotypes varies between different cells (Luduena, 1998). Microtubules in a given cell are co-polymers composed from available isotypes (Lopata and Cleveland, 1987). Isotypes demonstrate some functional significance in selective incorporation into labile and stable microtubules (Banjaree et. al, 1990; Luduena, 1993) Specific isotypes of tubulin share similar expression patterns with different MAPs including MAP1a, tau, MAP1b and MAP2 (Cowan et al., 1988; Oblinger and Kost, 1994). This suggests that different MAPs may interact preferentially with different tubulin isotypes. Tubulin isotype composition can influence microtubule dynamics *in vitro*. Microtubules demonstrate increases and decreases in microtubule polymerization depending on the tubulin isotype composition (Banerjee et al., 1990; Panda et al., 1994)

Heterogeneity of tubulin is further created by the modification of primary translation products (figure 5). Post translational modifications of tubulin include glutamylation, detyrosination, acetylation, glycylation and phosphorylation. α-Tubulin incorporated into a microtubule has tyrosine as its carboxy terminus end amino acid. During detyrosination of α-tubulin, the terminal tyrosine is removed from the carboxy end of α-tubulin by tubulin tyrosine carboxy peptidase. Detyrosination occurs preferentially on tubulin polymerized into microtubules. The longer a tubulin heterodimer remains incorporated in a microtubule, the greater chance of detyrosination. For this reason, detryosinated tubulin is correlated with increased stability and decreased turnover of

Figure 5: Illustration of post translational modification sites on α- and β-tubulin (Reproduced from Valliant 1997).

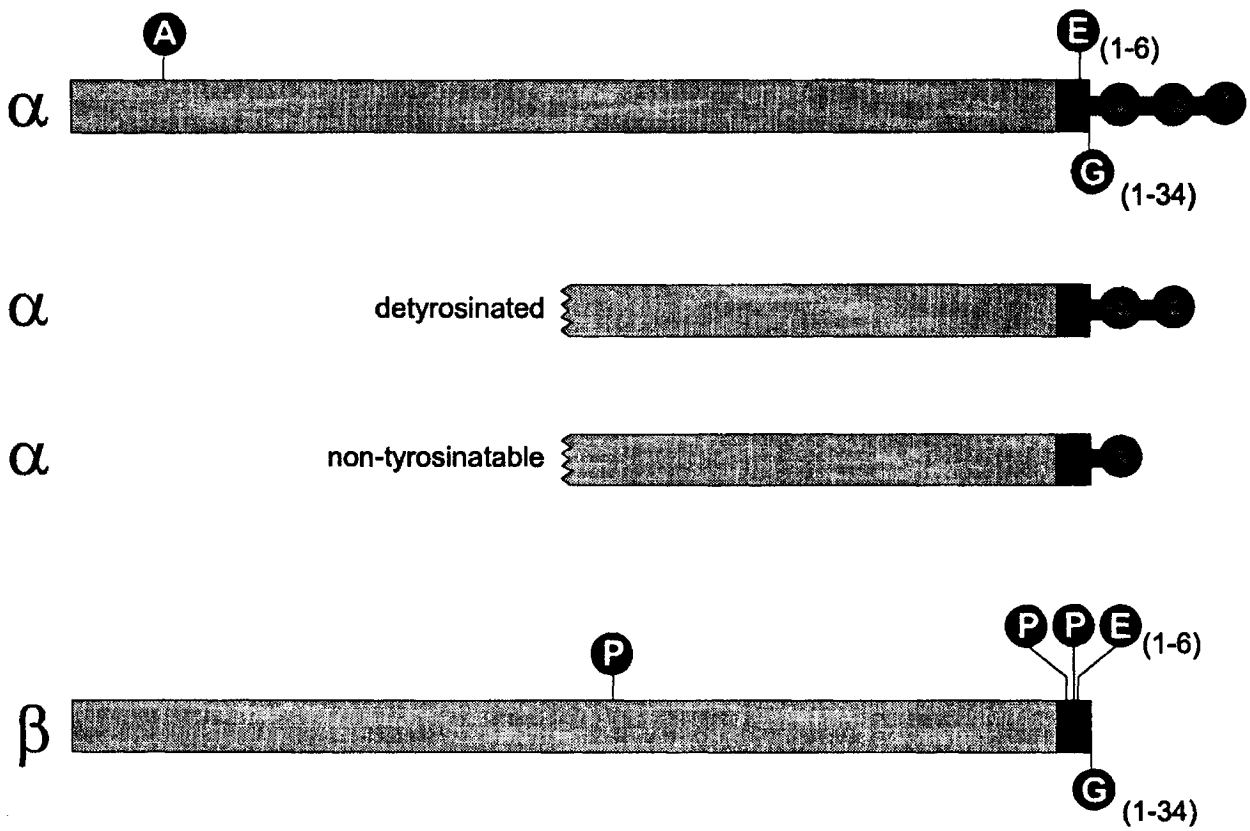

A = acetylation

E = glutamylation

G = glycylation

P = phosphorylation

■ = isotype defining region

microtubules. Microtubules that are highly detyrosinated are associated with an increased resistance to depolymerizing drugs (Khawaja et al., 1988). During shortening events heterodimers are released and the modification is reversed by the subsequent addition of tyrosine by tubulin tyrosine ligase (see figure 6). Elevated levels of detyrosinated α-tubulin have been detected in cells transfected with MAP1a, MAP2c and MAP1b (Takemura et al., 1992; Vaillant, 1998). Evidence suggests that detyrosination of tubulin may act as a signal for recruiting intermediate filaments to microtubules (Gurland and Gundersen, 1995; Kreitzer et al., 1999). Acetylation of α-tubulin at lys40 by acetyltransferase can also occur preferentially on polymerized microtubules. Highly acetylated microtubules are associated with decreased microtubule turnover and an increase in resistance to depolymerizing drugs (Schulze and Kirschner, 1986; Takemura et al., 1992).

Both tubulin subunits are subject to the reversible addition of 1-7 glutamyl units (Audebert et al., 1993; Regnard et al., 1998). Highly glutamylated microtubules are associated with an increase in resistance to depolymerizing drugs (Khawaja et al., 1988). α-tubulin glutamylation is relatively constant in both early and late development of neurons. The number of glutamyl residues attached to β-tubulin increases with development (Audebert et al., 1994; Redeker et al., 1996). This is similar to the developmental expression pattern of MAP1a. Differential polyglutamylation alters the binding affinity of tau, MAP1a, MAP1b and MAP2. Adult forms of highly polygluatmylated tubulin also display an enhanced affinity for MAP1a compared to other MAPs (Audebert et al., 1994; Boucher et al., 1994; Bonnet et al., 2001). This suggests

Figure 6: Schematic representation of the detryrosination and retyrosination of α-tubulin. During detyrosination of α-tubulin, the terminal tyrosine (t) is removed from the carboxy end of α-tubulin by tubulin tyrosine carboxy peptidase (TCP). Tubulin tyrosine ligase (T) replaces the terminal tyrosine on subunits that are released from microtuble ends.

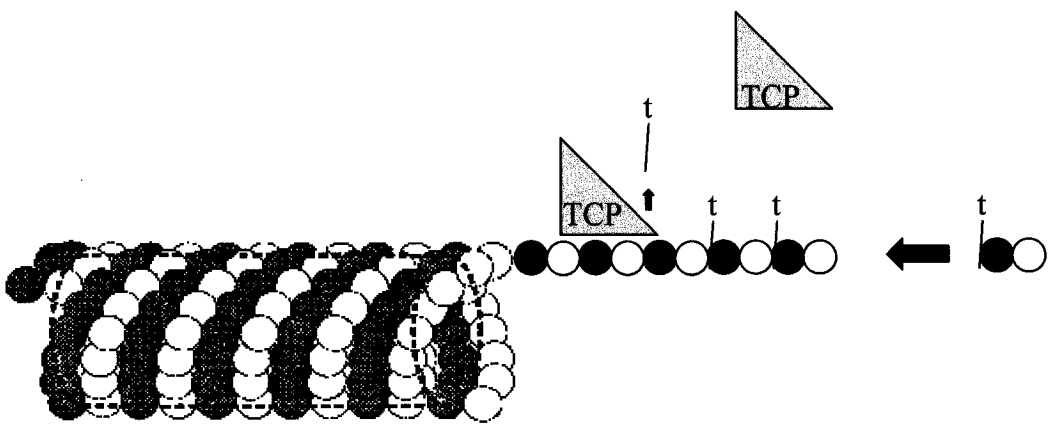
TCP
t
TCP
t
t
t

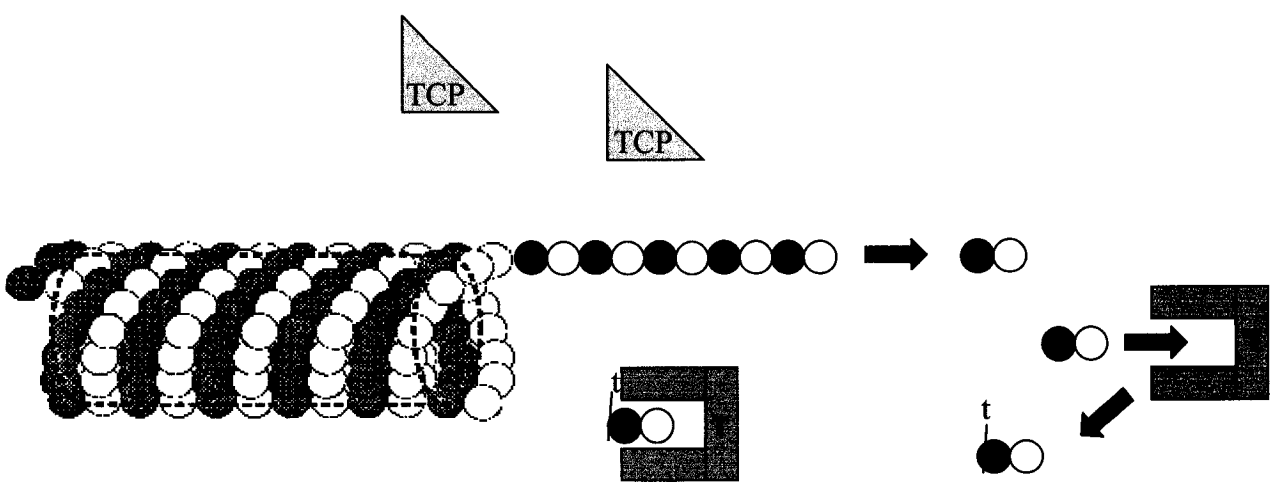
TCP
TCP
t
t

that variation in polyglutamylation could indirectly alter microtubule dynamics *in vivo* by altering the affinity of various MAP-microtubule interactions.

Alterations in the phosphorylation states of various tubulin isotypes can also alter microtubule dynamics. Phosphorylation of tubulin has been shown to modify growth and stability of microtubules *in vitro* (Wandosell et al., 1986; Khan and Luduena, 1996; Choudhary et al., 2001).

C. Microtubule-Associated Proteins

Structural microtubule-associated proteins (MAPs) are capable of interacting with tubulin dimers to regulate microtubule dynamics. MAPs share similar structural characteristics. MAP molecules contain a carboxy terminal microtubule binding and amino terminus projection domain (see figure 7). MAP bound microtubules require lower critical concentrations of soluble tubulin for microtubule assembly *in vitro*. MAP-microtubule binding also increases the frequency of rescue and decreases frequency of catastrophe events (Pryer et al., 1992; Cassimeris, 1993; Dhamodharan and Wadsworth, 1995). MAP2, MAP4, MAP1 and tau bind to the carboxy end of β-tubulin (see figure 8). The amino terminus of α-tubulin also contains a tau binding site (Littauer et al., 1986; Cross et al., 1991). The ability of MAPs to alter microtubule dynamics may be due to altering dimer association rates, affinity of tubulin for GTP, or formation of cross bridges with cytoskeletal elements (Takemura et al., 1992). MAP1a, MAP1b, MAP2, MAP4, and tau are the best-characterized structural MAPs (see tables I and II).

Figure 7: Model of MAP association with microtubules (Reproduced from Valliant 1997).

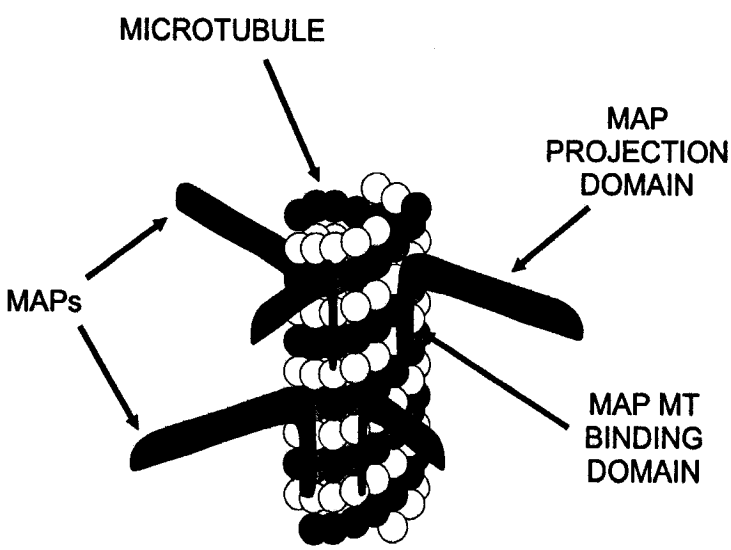
MICROTUBULE
MAP
PROJECTION
DOMAIN
MAPs
MAP MT
BINDING
DOMAIN

Figure 8: Location of MAP binding sites present on α- and β-tubulin (Reproduced from Valliant 1997).

TAU *

MAP1A *
MAP1B *
MAP2 *
MAP4 *
TAU *

■ = isotype defining region

Table I: MAP isoforms of the nervous system: localization, and expression (adapted from Riederer, 1990, Doll et al., 1993 and Schoenfeld and Obar, 1994).

Species	Isoforms*	MW (kDa)	Nervous System Localization	Expression During Neuronal Differentiation
MAP1A		350	dendrites, soma & axons	late
MAP1B		330	dendrites, soma & axons	early
MAP2	MAP2a	280	dendrites & soma	late
	MAP2b	260	dendrites & soma	early & late
	MAP2c	70	dendrites, soma & axons	early
	MAP2d	74	glial cells	late
tau	multiple (6)	45-65	preferentially in axons	early (juvenile forms) late (adult forms)

*They are generated by alternative mRNA splicing

Table II: The two principal structural MAP families.

Family	MT -Binding Domain	Reference
Tau-MAP2-MAP4	- located near C-terminus of each molecule;	
	- consists of two regions:	
	1) three to four 18-amino acid repeats;	Gustake et al., 1994;
	2) the regions flanking these repeats	Goedert et al., 1996.
MAP1	- located near N-terminus of each molecule;	
	- consists of two regions:	
	1) eleven /twenty-one repeats of (K/R) (K/R) (E/D) motif ;	Noble et al. ,1989;
	2) the regions flanking these repeats	Vaillant et al.,1998.

All of these structural MAPs (except MAP 4) are predominantly found in neurons. Structural MAPs appear to modulate microtubule dynamics by ionically binding to microtubules to promote stability and elongation (Avila et al., 1994; Dhamodharan and Wadsworth, 1995). Several MAP kinases are associated with phosphorylation of the MAP1 family (Fujii et al., 1996; Ramon-Cuento and Avila, 1999). MAP-microtubule binding appears to be controlled by phosphorylation and dephosphorylation of MAPs at serine and threonine residues. MAP phosphorlyation is executed by various protein kinases and phosphatases (Brugg and Matus, 1991; Gordon-Weeks, 1993; Avila et al., 1994; Gong et al., 2000). Phosphorylation of MAP1b is developmentally and spatially regulated in neurons and varies between different cell types (Sato-Yoshitake et al., 1989; Pedrotti and Islam, 1996a; Ramon-Cuento and Avila, 1999)

C.1. MAP4

MAP 4 family proteins contain repeated amino acid sequences similar to MAP2 and tau microtubule binding domains (MacRae, 1992). MAP4 has been shown to cross-link and bundle microtubules *in vitro*. GFP- tagged MAP4 molecules colocalize with microtubules, and induce bundling and stabilization of microtubules. MAP4 has assembly-promoting regions at its carboxy end. These assembly promoting regions are regulated by phosphorylation of amino acid residues in the proline rich region of the MAP4 carboxy terminus. The projection domain of MAP4 appears to regulate the interaction of the binding domain with microtubules (Olson et al., 1995).

C.2. Tau

Tau is one of the earliest discovered and best-characterized MAP. Developmentally regulated alternative splicing of the same mRNA product results in six different isoforms of tau. Tau is concentrated in distal regions of growing axons. Tau displays similar functions to MAP1b in the ability to promote neuron process emergence and axonal elongation. The abilities of tau to promote growth and nucleate microtubules involve separate regions of the protein (Brandt and Lee, 1993). The carboxy terminus of tau is responsible for binding to microtubules (Himmler et al., 1989). Regions flanking binding sites boost binding affinity dramatically (Gustake et al., 1994; Frappier et al., 1994). *In vitro* microtubule polymerization studies have shown that tau increases microtubule growth 2-3 fold and protects microtubules from shrinking and catastrophe events (Geodert and Jakes, 1990; Trinczek at al., 1995). In transfected cells, tau colocalizes with microtubule bundles that are resistant to colchicine treatment (Lo et al., 1993).

C.3. MAP2

MAP2 proteins are capable of binding to microtubules, intermediate filaments and actin as determined by *in vitro* binding and colocalization studies (Bloom and Valee, 1983; Sattilaro, 1986). MAP2a and MAP2b are predominant in dendrites of mature neurons. MAP2c is expressed throughout immature neurons. (Crandall and Fischer,

1989; Harrison and Hyams, 1990). MAP 2 isoforms are produced by the alternative processing of the same gene product. The carboxy terminal region of MAP2 contains 18 amino acid repeats associated with the binding and microtubule polymerization-promoting abilities of MAP2 proteins (Lewis et al., 1988; Harrison and Hyams, 1990). Binding of MAP2 proteins to microtubules induces bundling and stiffening of microtubules (Weisshaar et al., 1992; Weisshaar and Matus, 1993; Kalcheva, 1998). Bundling of microtubules may be an indirect outcome from increased microtubule stability (MacRae, 1992). In the presence of MAP2, microtubules are resistant to drug-induced depolymerization. Microtubules bound to MAP2 resist depolymerization better than tau bound microtubules (Fellous et al., 1994). This suggests that MAP2 is a stronger stabilizer of microtubules compared to tau. MAP2 proteins have been shown to decrease the frequency of dynamic event transitions and increase the amount of time microtubules spend in pause (Dhamodharan and Wadsworth, 1995)

MAP2c induces bundling, stiffening and stabilization of microtubules when expressed in non-neuronal cells. MAP2c is a rod shaped molecule capable of self-association into antiparallel dimers, which may be responsible for the bundling properties of MAP2c (Wille et al., 1992). MAP2c has been shown to stabilize microtubules *in vitro* by suppressing dynamic instability (Gamblin et al., 1996). MAP2c bound microtubules have fewer transitions between growth and shortening phases, microtubule growth and shortening are both inhibited, and microtubules spend an increased time in an attenuated state.

C.4. MAP1 Family

The MAP1 family includes two proteins: MAP1a and MAP1b (see figure 9). These proteins share similarities in sequence and charge distribution (Langkopf et al., 1992). Shared sequences are found predominantly at the carboxy and amino ends of MAP1. The microtubule-binding site of MAP1a appears to be present near the amino terminus of the protein and is characterised by a KKE repeat motif of 11 repeats. A similar 21 KKE repeat motif, which has also been implicated in binding to microtubules, is present in MAP1b (Noble et al., 1989; Langkopf et al., 1992). The repeat region of MAP1a is bounded by two flanking regions that also play a role in microtubule binding. Flanking regions may possess greater binding affinity in the absence of the basic repeat region (Vaillant et al. 1998).

MAP1a and MAP1b expression are most prominent in the brain (Bloom et al., 1985; Fukuyama and Rapoport, 1995; Fink et al., 1996). MAP1a and MAP1b are developmentally regulated. Levels of MAP1a in rats increase with neuronal development and MAP1b decreases (Oblinger and Kost, 1994). This correlation suggests that MAP1a may be replacing MAP1b as the neuronal cells develop. Maturation of neurons is characterised by a decrease in neuronal process growth and the stabilization of mature brain circuitry.

MAP1a is present in the neuronal cell body, axons and dendrites. MAP1b is predominant in axons and dendrites and is particularly concentrated in axonal growth cones (Bloom et al., 1985; Black et al., 1994). In growth cones MAP1b is involved in

Figure 9: Illustration of proteins in the MAP1 family and their associated light chains (Reproduced from Valliant 1997).


MAP1a
1
2774
LC2
LC2
MAP1b
1
2464
LC1
LC1
= basic repeat
= flanking domains
= acidic repeat
1
142
LC3

neurite initiation, outgrowth and the formation of neuronal processes (Brugg et al., 1993; Mack et al., 2000) The phosphorlyated form of MAP1b is particularly important in these events (Gordon-Weeks, 1993; Fink et al., 1996). MAP1a is also present in areas of plasticity and has been shown to promote microtubule assembly (Pedrotti et al., 1993; Pedrotti and Islam 1994). *In vitro* experiments have demonstrated an increase in microtubule assembly and rates compared to unbound microtubules. *In vivo* studies have also demonstrated the growth promoting ability of MAP1a in dendrites (Ferria et al., 1989). MAP1b also promotes microtubule polymerization *in vitro* without bundling microtubules. MAP1b demonstrates an increased ability to promote microtubule polymerization compared to MAP1a (Pedrotti and Islam, 1995). MAP1a can also bind to actin to cross-link actin filaments, but with three times less affinity than MAP2. This may be important by allowing for a more dynamic interaction between microtubules and actin filaments (Pedrotti et al., 1994; Fujii et al., 1993) MAP1a has a projection domain whose role remains unclear. The projection domains of some MAPs have been implicated in the regulation of the activity of the microtubule-binding domain (Olson et al., 1995). Additional evidence suggests that spacing, bundling and cross-linking of microtubules in axons and dendrites may be determined by the projection domain (Chen et al., 1992).

C.5. MAP1 Associated Light Chain Molecules

The MAP1a heavy chain molecule is associated with three light chains (Vallee and Davis, 1983; Kuznetsov et al., 1986; Kuznetsov and Gelfland, 1987). LC1 (27 kDa) is encoded within the 3' end of MAP1b (Hammarback et al., 1991). LC2 (24 kDa) is encoded within the 3' end of MAP1a (Langkopf et al., 1992). Both LC1 and LC2 are post-translationally cleaved from their respective MAP1 heavy chains by selective proteolysis (Hammarback et al., 1991; Langkopf et al., 1992; Togel et al., 1998) (see figure 10). LC 3 (19 kDa), on the other hand, is encoded in a distinct gene (Mann and Hammarback,1994; Mann and Hammarback, 1996). Although not present in the same gene, LC3 is always co-expressed with either MAP1a or MAP1b (Mann and Hammarback, 1996). Light chain molecules bind to the amino terminus of MAP1 heavy chain molecules, near the microtubule binding domain (Kuznetsov et al., 1986; Schoenfeld et al., 1989; Muller et al., 1994; Mann and Hammarback, 1994). The phosphorylation of MAPs does not appear to influence the ability of light chains to bind to heavy chain molecules (Pedrotti et al., 1995). LC3 appears to promote association of heavy chains to microtubules (Mann and Hammarback, 1994). Association of light chain molecules with MAP1a and MAP1b may alter their ability to bind microtubules and alter microtubule dynamics (Schoenfeld et al., 1989; Mann and Hammarback, 1996). Light chain effects on microtubules appear to be regulated by heavy chain molecules. Expression of heavy chain with light chains appears to inhibit the ability of light chains to alter microtubule

Figure 10: Proteolytic processing of proteins in the MAP1 family resulting in functionally active heavy and light chains from polyprotein precursors (Reproduced from Muller et al., 1994).

MAP1 - LIGHT CHAIN PROCESSING

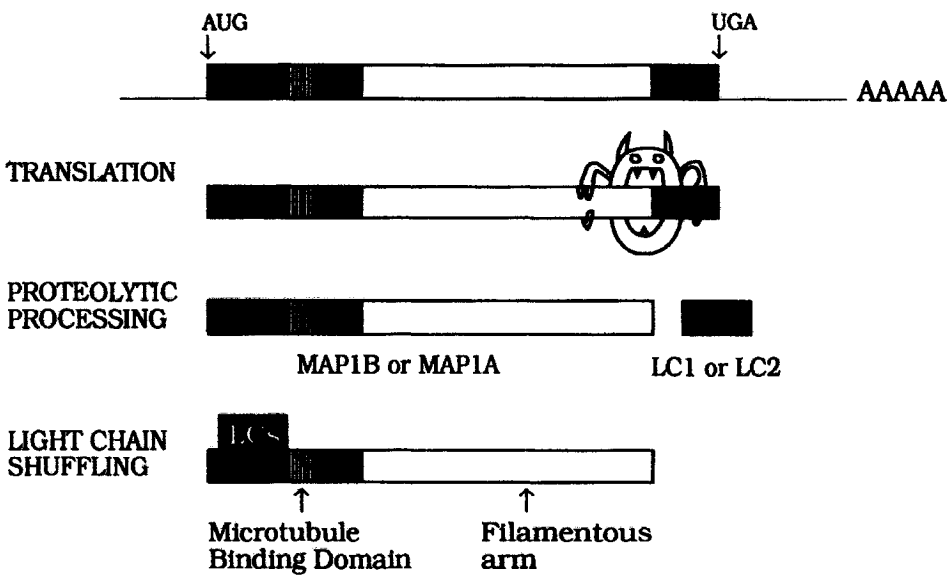

organization, stability and their ability to bind on actin filaments (Togel et al., 1998; Villeneuve, 2003).

Light chain molecules have been detected at stoichiometries of 6-8 fold compared to their respective heavy chains. Light chain molecules have been detected in non-neuronal cells and may be expressed in the absence of heavy chain molecules. This suggests that light chain molecules have functions in addition to their association with MAP1 heavy chains (Mei et al., 2000). LC1, LC2 and LC3 are capable of binding to microtubules in the absence of MAP1 molecules. Light chain and heavy chain molecules colocalize on the same microtubules *in vivo*.

The binding of LC1 and LC2 to microtubules reorganizes microtubules into wavy bundles. LC1 and LC2 also increase the resistance of microtubules to depolymerizing drugs (Togel et al., 1998, Ungureanu, 2002, Noiges et al., 2002). Both LC1 and LC2 promote tubulin polymerization *in vitro*. Oligmerization of LC1 through association of its carboxy terminus domains may promote microtubule growth by recruiting tubulin to polymerized microtubules (Noiges et al., 2002).

D. Rationale For Experiments

MAP1a is the predominant MAP in the adult brain . (Fukuyama and Rapoport, 1995; Fink et al., 1996). The fact that MAP1a is expressed at high levels in all regions of the adult brain suggests that MAP1a is important to proper development and maintenance of neuronal tissue. The adult stage of neuronal development is associated with the

stabilization of mature brain circuitry and increased microtubule stability (Oblinger and Kost, 1994; Fukuyama and Rapoport, 1995). However, MAP1a does not bundle microtubules and it does not stabilize microtubules against depolymerizing drugs *in vitro* or *in vivo*. The ability of MAP1a to promote microtubule growth *in vitro* is less than other MAP proteins such as tau, MAP2 and MAP1b. MAP1a associated light chains reorganize microtubules into wavy bundles and stabilize microtubules against deploymerizing drugs. This suggests that light chain molecules may alter microtubule dynamics *in vivo*. In spite of the predominant nature of MAP1a in the mature brain, little is known about how MAP1a and its associated light chains affect microtubule dynamics *in vivo*.

Vaillant et al., (1998) have constructed 6myc tagged fragments of MAP1a and its three associated light chains. The 6myc tagged light chains and MAP1a fragments that contain the basic repeat and/or flanking regions bind to microtubules *in vivo*. These fragments vary in their ability to stabilize microtubules (measured by increases in detyrosinated tubulin levels). This suggests that these fragments vary in their ability to modulate microtubule dynamics.

We have obtained the mammalian cell line LLC-PK1α that has been stably transfected with α-tubulin-GFP. Green Fluorescent Protein (GFP) is a 238 aa protein that has been used to tag a wide range of cytoskeletal proteins without altering protein behaviour (Ludin and Matus, 1998). The ability of GFP to be detected *in vivo* and the ability to resist photobleaching make GFP well suited for observations of cytoskeletal dynamics (White and Stelzer, 1999). The GFP fluorophore is relatively benign, with

limited free radical production, probably due to the fact that the fluorophore is tightly confined in a barrel structure of the protein (Ludin and Matus, 1998; Ikawa et al., 1999). 17% of the tubulin present in the permanently transfected LLC-PK1α cell line is GFP-α-tubulin. However, the amount of total tubulin is similar in LLC-PK1α and wild type cells showing that the expression of α-tubulin-GFP does not increase the amount of tubulin in the cell. The LLC-PK1α cell line also demonstrated microtubule dynamic behaviour similar to wild type LLC-PK1 cells (Rusan et al., 2001) indicating that the GFP tag does not interfere with microtubule dynamics.

The goal of this study is to make direct measurements of microtubule dynamics in living cells that are transiently expressing MAP1a and light chain fragments. These observations are expected to show the impact of MAP1a and its associated light chain molecules on microtubule dynamics *in vivo*.

II. MATERIALS AND METHODS

A. MAP1a and MAP2c Expression Constructs

The PGK-6myc MAP1a heavy chain fragment expression vectors (figure 11) were constructed by Andrew Vaillant using three overlapping cDNAs spanning the entire mRNA for MAP1a, including light chain 2 (Langkopf et al., 1992,Vaillant et al., 1998). Coding sequences for the full length MAP1a and MAP1a heavy chain fragments were cloned into the pKJ1ΔF-6myc vector, a gift from Dr. M. McBurney (University of Ottawa). pKJ1ΔF-6myc is a PUC19-based vector containing the constitutively active mouse phosphoglycerate kinase (PGK) promoter driving the expression of 6 repeats of a 9 amino acid epitope from the human c-MYC protein.

The pPGK-MAP2c plasmid was constructed by C.Addison (1997) from our laboratory. The pPGK-MAP2c expression vector was constructed by ligating a 1.7kb fragment containing the MAP2c cDNA (Kindler et al., 1990) (a gift from Dr.C.Garner, University of Alabama, Birmingam) into the pKJ1ΔF-6myc plasmid.

The PGK-6myc light chain (LC1, LC2, and LC3) expression vectors were also constructed by Andrew Vaillant (1998). For LC1 a 753 bp Nco1- EcoR1 fragment corresponding to light chain 1 (Hammarback et al., 1991), for LC2 a Nco1- EcoR1 666 bp fragment corresponding to the region for light chain2 (Langkopf et al., 1992) and for

Figure 11: PGK 6myc tagged expression constructs of truncated MAP1a and its associated light chains, built by Vaillant (1997).

* Molecular weight does not include LC2

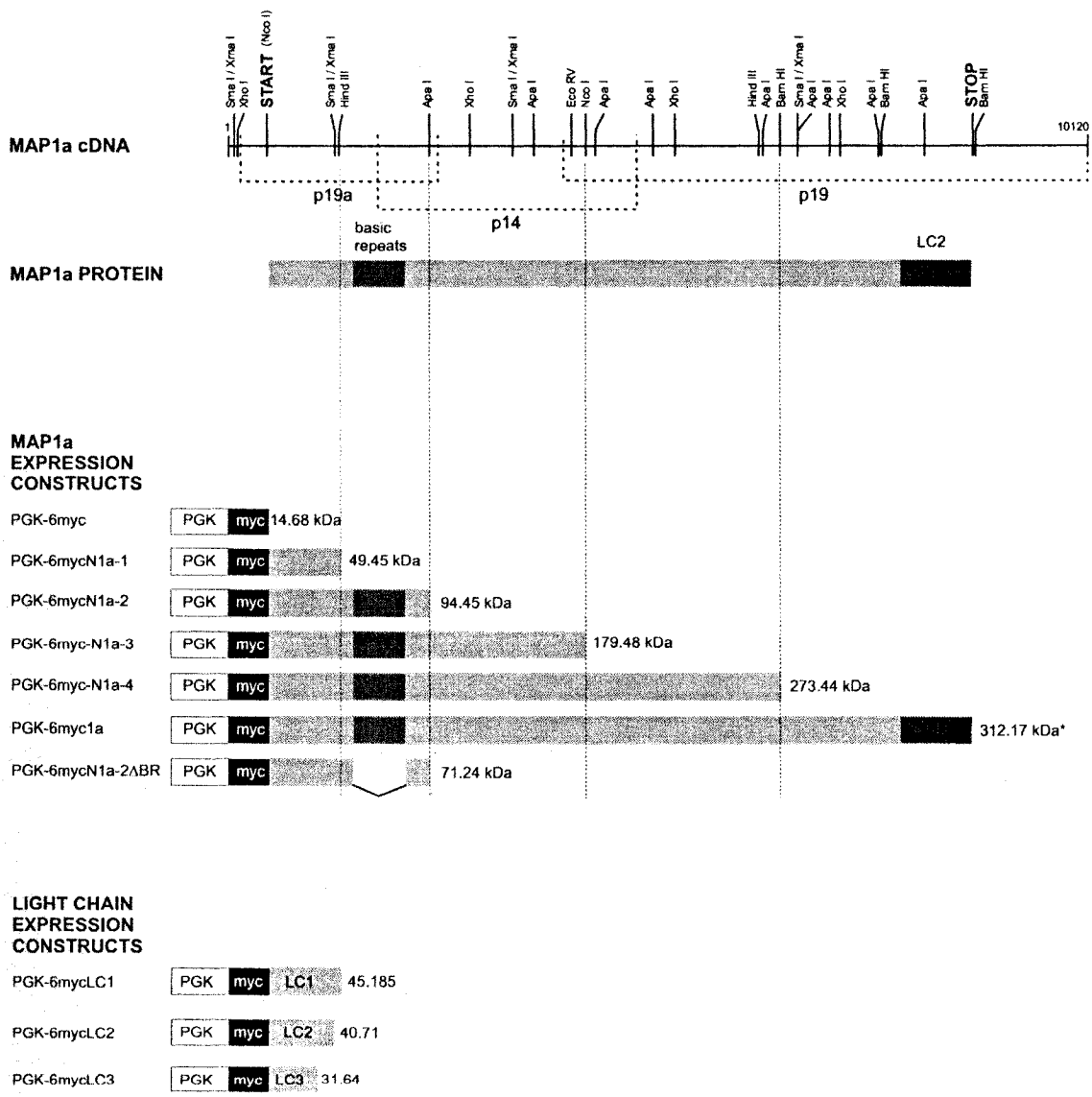
MAP1a cDNA
Sma I / Xma I
Xho I
START (Nco I)
Sma I / Xma I
Hind III
Apa I
Xho I
Sma I / Xma I
Apa I
Eco RV
Nco I
Apa I
Apa I
Xho I
Hind III
Apa I
Bam HI
Sma I / Xma I
Apa I
Apa I
Xho I
Apa I
Bam HI
Apa I
STOP
Bam HI
1
10120
p19a
p14
p19
basic repeats
LC2
MAP1a PROTEIN
MAP1a EXPRESSION CONSTRUCTS
PGK-6myc
PGK
myc
14.68 kDa
PGK-6mycN1a-1
49.45 kDa
PGK-6mycN1a-2
94.45 kDa
PGK-6myc-N1a-3
179.48 kDa
PGK-6myc-N1a-4
273.44 kDa
PGK-6myc1a
312.17 kDa*
PGK-6mycN1a-2ΔBR
71.24 kDa
LIGHT CHAIN EXPRESSION CONSTRUCTS
PGK-6mycLC1
LC1
45.185
PGK-6mycLC2
LC2
40.71
PGK-6mycLC3
LC3
31.64

LC3 a 818 bp Nde-EcoR1 fragment corresponding to LC 3 (Mann and Hammarback, 1994) were blunt end ligated into the pKJ1ΔF-6myc vector.

B. Large Scale Production of Plasmid DNA

Plasmid DNA was transformed into competent DH5αF′ *E. coli.*, and grown overnight at 37°C on Luria Bertani broth plates augmented with 100ug/ml kanamycin (GFP plasmids) or 100ug/ml Ampicillin (PGK-6myc plasmids). Colonies were removed and used to inoculate 5 ml of LB cultures with either 100ug/ml kanamycin, or 100 µg/ml ampicillin, as above. Cultures were grown for 8 hours at 37°C, with vigorous shaking (~300 rpm). 5ml cultures were diluted 1:500 in 500 ml LB-broth with kanamycin or with ampicillin, as above, and grown for an additional 8 hours. Plasmid DNA was harvested from these large cultures by centrifugation and isolated by alkaline-lysis using the Qiagen Plasmid Mega kit (25) (Qiagen). Recovered plasmid was dissolved in ddH_2O and stored at -20°C. DNA concentration and purity were determined by UV absorbency at 260 and 280nm using a Genequant® spectrophoto-meter (Pharmacia).

C. LLC-PK1α Cell Line

We obtained a mammalian cell line (LLC-PK1) which has been permanently transfected with human α tubulin-GFP (clonetech) from Dr. Patricia Wadsworth (University of Massachusets) (figure 12). 17% of the tubulin present in this transfected

Figure 12: Detection of α-tubulin:GFP in LLC-PK1 α cells by fluorescence microscopy. Cells were housed in a Dvorak-Stotler live cell observation chamber Scale bar = 10 μm.

cell line is GFP-tubulin. The LLC-PK1α cell line has similar total concentration of tubulin compared to wild type LLC-PK1 cells (Rusan et al., 2001). This cell line demonstrated microtubule dynamic behaviour similar to that in wild type LLC-PK1 cells. LLC-PK1 cells are derived from pig kidney epithelium and are capable of growing in a monolayer, suitable for microscopic observation.

D. Tissue Culture and Transient Transfection

LLC-PK1α cells (ATCC) were kept semiconfluent in Eagle's minimal essential medium α (GIBCO BRL) supplemented with 10% FCS (Cansera), O.85g/L sodium bicarbonate (GIBCO), 0.12g sodium pyruvate (GIBCO) and 1% antibiotics (GIBCO). Cells were grown in a humidified incubator at 37°C and 5% CO_2 and passed every two days. Every second week, media was supplemented with 200mg/L of G418 sulfate (Geneticin) for 48 hours to select for cells expressing GFP-α tubulin. The day before transfection, cells were seeded on 22 mm^2 glass coverslips (VWR) at a density of $5x10^4$ cells/ml, for microscopy, or on 60 mm culture dishes (Corning) at a density of $5 x10^5$ cells/ml, for protein extraction. Cells were allowed to recover for 24 h in MEM (0.12g sodium pyruvate, O.85g/L sodium bicarbonate) containing 10%FCS and 1% antibiotics. For transfection experiments, cells were transiently transfected with DNA using Maxfect liposomal reagent (Molecula Research), followed by application of Booster Reagent #2 (Gene Therapy Systems).

E. SDS- Whole Cell Protein Extraction

This method (figure 13) was used for preparing extracts for SDS-PAGE analysis. Protein was extracted from cells using the method described in Drubin et al., (1985), but using higher concentration of protease inhibitors in the extraction buffer. Cells were washed briefly in rinse buffer [0.13M NaCl, 2mM KCl, 8mM Na_2HPO_4, 2mM KH_2PO_4, pH7]. 250µl of extraction buffer [25mM Na_2HPO_4, pH 7.2, 400mM NaCl, 0.5%(w/v) SDS, 40 µM benzamidine HCl (Sigma), 4 mM PEFA (Centrichem), 1mM 1,10-phenathroline (Sigma), 40 µg/ml each of apoprotinin, pepstatin A and leupeptin (all from Sigma)] was added. The viscous lysate was immediately scraped into an eppendorf tube and placed in a boiling water bath for 10 min followed by centrifugation for 10 min at 10 000 rpm and 4°C. The supernatant containing extracted proteins was removed and stored at -85°C. Protein concentrations were determined using the bicinchoninic acid protein assay (Pierce) with Bovine Serum Albumin (Pierce) diluted in ddH2O as a standard.

F. SDS-PAGE and Western Blotting

Protein samples (1:1dilution) and a biotinylated SDS-PAGE broad range standard (1:10 dilution) (BioRad) were diluted as specified in 2x sample buffer (Laemmli, 1970). Samples were boiled for 5 min, and loaded onto 7.5 % polyacrylamide gels. Proteins were separated using the BioRad minigel apparatus. After separation, proteins were

Figure 13: SDS-whole cell extraction protocol

(Reproduced from Valliant 1997).

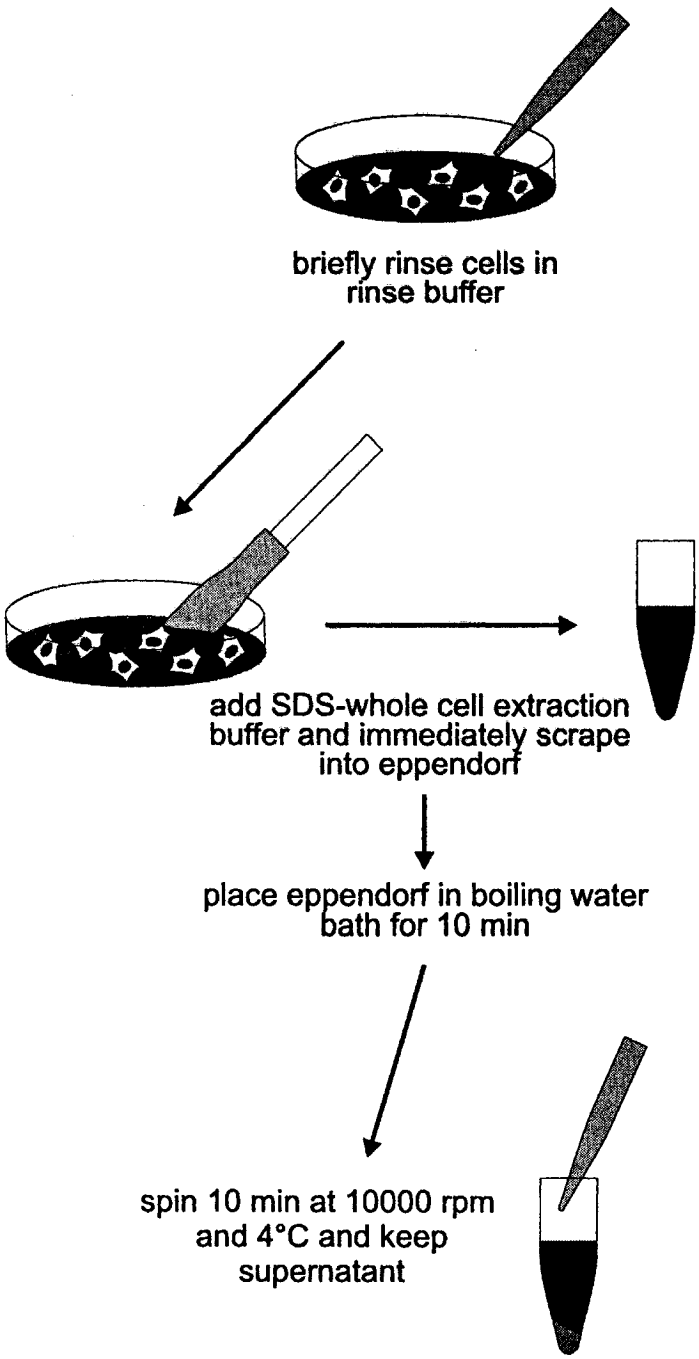
briefly rinse cells in rinse buffer
add SDS-whole cell extraction buffer and immediately scrape into eppendorf
place eppendorf in boiling water bath for 10 min
spin 10 min at 10000 rpm and 4°C and keep supernatant

electrotransferred overnight onto nitrocellulose (NS)(Scleicher and Scheull) according to Towbin et al., 1979. Nitrocellulose blots were rinsed in PBS and processed for western blotting. First, the blots were incubated at 4°C for 1 hr in 5% (w/v) skim milk (Carnation) in PBS containing 0.05% Tween. This was followed by a 1-hr incubation in primary antibody diluted in 2% skim milk in PBS-Tween. The blots were then washed 3x5 min in PBS-0.05%Tween. Blots incubated with the mouse monoclonal antibodies for anti-6myc or anti-tubulin were then incubated for 45 min in biotinylated horse anti-mouse polyclonal secondary antibody diluted in 2% skim milk followed by 3x5min washes in PBS-0.05%Tween. Blots were then incubated for 30 min in streptavidin-HRP (Amersham) diluted 1:5000 in PBS. Blots incubated with the rabbit polyclonal antibody for anti-detryosinated αtubulin were then incubated for 45 min in biotinylated goat anti rabbit polyclonal secondary antibody diluted in 2% skim milk followed by 3x5min washes in PBS-0.05%Tween. Blots were then incubated for 30 min in streptavidin-HRP (Amersham) diluted 1:5000 in PBS. For all blots, antibody binding was detected by enhanced chemiluminescence (ECL) (Amersham) using Hyperfilm–ECL (Amersham). Films were digitized at 400 dpi using a Hewlett-Packard 4c flatbed scanner. Digitized TIFF images were then processed using Adobe Photoshop v4.0 and Powerpoint 97 (Microsoft). Quantification of protein bands by optical density was performed with metamorph ver. 4.0 software.

G. Fluorescence Microscopy

Cells grown on coverslips were briefly rinsed in PEM buffer and fixed by two different methods:

1) Extraction/fixation: Cells were pre-extracted for 2min in 0.2% Triton X-100 in PEM buffer. Cells were then simultaneously fixed and extracted for 10 min in 3.7% paraformaldehyde (v/v) (BDH), 0.25% glutaraldehyde (v/v) (JB EM Services Inc.) and 0.5% Triton X-100 (v/v) in PEM buffer (Falconer et al., 1992). Finally, coverslips were washed 3x5 min in PBS.

2) Precipitation fixation (Steffanini et al., 1967): cells were incubated for 1 hour in a fixative solution containing 14% picric acid (Fisher), 4% paraformaldehyde (JB EM Services Inc.) in 0.5M Na_2HPO_4, 0.5M NaH_2PO_4, pH 7.1 Cells were then washed 3x5 min with PBS, followed by a 5 min extraction with 0.5% Triton X-100 in PBS, and final 3x5 min PBS washes.

Double immunofluorescence labeling was performed sequentially, in a humid chamber, at room temperature. Before primary antibody incubation, cells were incubated for 3x4 min with 1mg/ml $NaBH_4$ (BDH) in PBS, to reduce free aldehyde groups, and then rinsed again 3x5 min in PBS. All antibody incubations were for 1 hour with 3x5min PBS washes after each incubation, with the exception of the anti-detyrosinated α-tubulin antibody incubation (20 min). Cells were then mounted in

Vectashield mounting medium (Vector Laboratories Inc) and visualized with a Zeiss Universal epi-fluorescence microscope equipped with a 50 W Hg burner. Images were digitally recorded with a Hamamatsu integrating CCD camera using Metamorph v 4.0 software (Universal Imaging). All images were saved as TIFF files and were processed using Adobe Photoshop v. 4.0 and Powerpoint 97 (Microsoft).

H. Antibodies

Anti- α-Tubulin

Mouse monocolonal IgG1 isotype [clone DM 1A (Sigma)] used at 1:1000 for immunoblotting.

Anti-Detyrosinated α-Tubulin

rabbit polyclonal Ig (anti-E, Xiang and MacRae, 1995) provided by Dr.T.MacRae (Dalhousie University, NS) and used at 1:250 for immunolabelling, and 1:1000 for immunoblotting.

Anti-MAP1A

mouse monoclonal IgG1isotype [clone HM-1 (Sigma)] was used at 1:500 for immunoblotting.

Anti-MAP1B

Mouse monoclonal 1gG [clone AA6 (Sigma)] used at 1:300 for immunoblotting.

Anti-MAP2

Mouse monclonal IgG [clone HM-2 (Sigma)] used at 1:500 for immunoblotting.

Anti-Tau

Mouse monoclonal IgG (clone Tau-2, Papasosomenos and Binder, 1987) provided by Dr. L. Binder, used at 1:1000 for immunoblotting.

Anti-6Myc Tag

Mouse monoclonal IgG (clone 9E10, Evan et al., 1985) provided by Dr. C. Garner (University of Alabama, AL) and used undiluted for single and double immunolabelling.

Anti-Mouse IgG

Donkey polyclonal IgG (H+L) conjugated to indocarbocyanine (CY3) (Jackson), crossadsorbed to rat and rabbit used at 1:400 for immunofluorescence microscopy.

Alexa 350 Goat-anti mouse monclonal IgG (H+L) conjugate (Molecular Probes), used at 1:200 for immunolabelling.

Horse polyclonal IgG, biotinylated (Vector) and used at 1:1000 for immunoblotting.

Anti-Rabbit IgG

Donkey polyclonal IgG (H+L) conjugated to indocarbocyanine (CY3)(Jackson) used at 1:400 for immunofluorescence microscopy.

Polyclonal goat IgG, Biotinylated (Dimension) used at 1:1000 for immunoblotting.

Anti-light chain 1

Mouse monoclonal IgG [clone E12 (Sigma)], used at 1:1000 for immunoblotting.

I. Live Cell Methodology

Cells were co-transfected (figure 14) with 2.0μg of one of the 6myc tagged MAP1A fragments (described above) and 0.5μg of the dsRed plasmid (Clonetech). Cells were transiently co-transfected with DNA using the Maxfect liposomal reagent (Molecula Research),

followed by application of Booster Reagent #2 (Gene Therapy Systems). After a 24 hour recovery period, cells were trypsinized and re-seeded on round, 22mm photo etched coverslips (Electron Microscopy Sciences). After 24 hours of growth on photoetched coverslips (they have a grid co-ordinate system), cells were placed in a closed Dvorak-Stotler live cell observation chamber with a 2020 technologic stage heater. The grid co-ordinates on the photo etched coverslips were recorded for cells expressing DsRed. Once the grid co-ordinates and dsRed expression were recorded, cells were observed to collect live cell data to quantify their microtubule dynamic behaviour. Observation of LLC-PK1α microtubule ends was performed using a Zeiss Axiophot epi-fluorescence microscope (equipped with a Z-axis stage motor). Two-second exposures were taken every 4 seconds over a 2-minute period. A Hamamatsu chilled 8-bit black and white CCD camera and Metamorph ver. 4.0 software were used to capture and process images. Once live cell measurements were recorded for cells in which the DsRed plasmid was detected, cells were immediately fixed by the precipitation protocol. Cells were then immunolabeled with a mouse monoclonal anti-6myc primary antibody 9E10 followed by a secondary monoclonal anti-mouse Alexa

Figure 14: Illustration of protocol to measure microtubule dynamics *in vivo*.

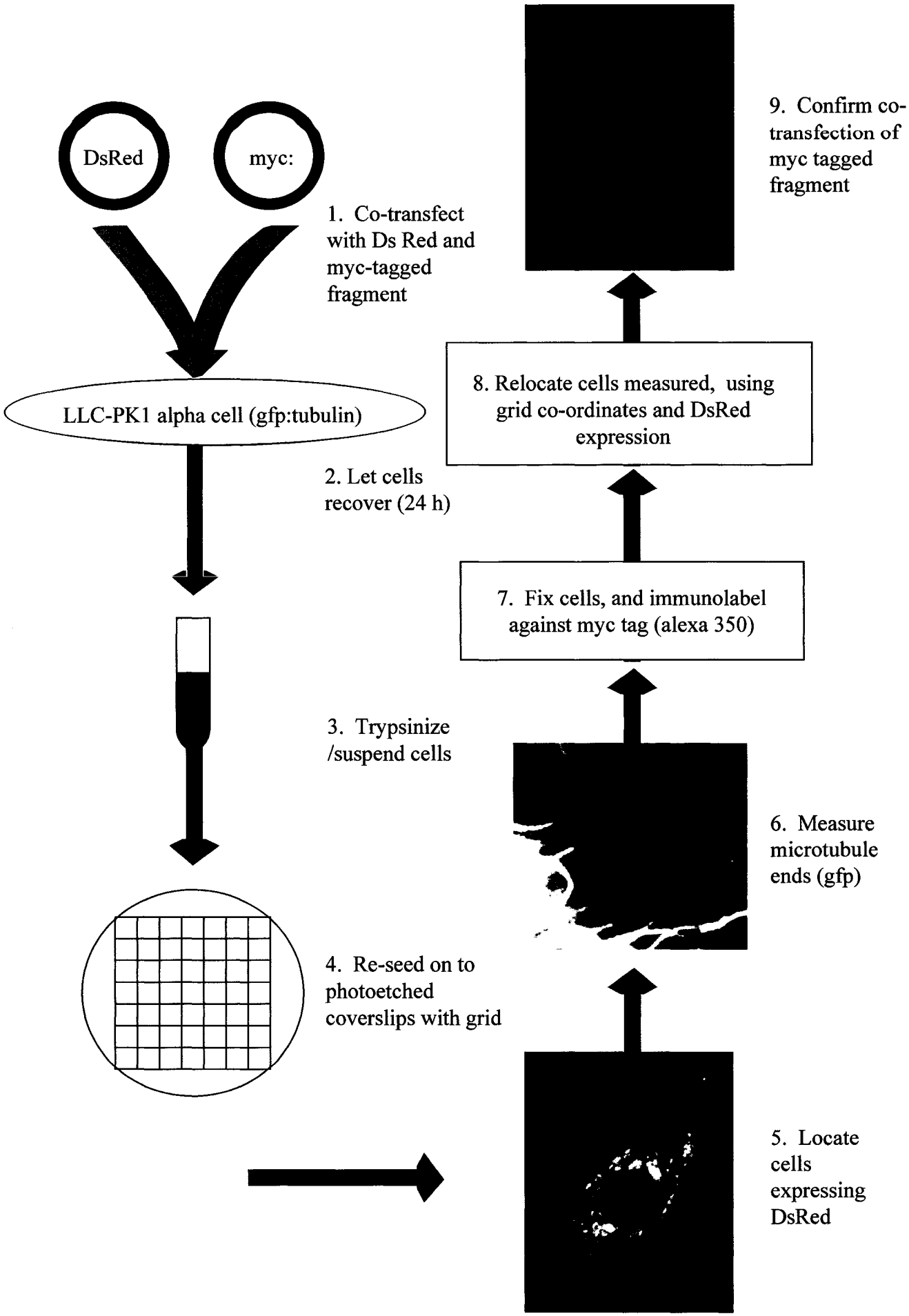
DsRed
myc:
1. Co-transfect with Ds Red and myc-tagged fragment
LLC-PK1 alpha cell (gfp:tubulin)
2. Let cells recover (24 h)
3. Trypsinize /suspend cells
4. Re-seed on to photoetched coverslips with grid
5. Locate cells expressing DsRed
6. Measure microtubule ends (gfp)
7. Fix cells, and immunolabel against myc tag (alexa 350)
8. Relocate cells measured, using grid co-ordinates and DsRed expression
9. Confirm co-transfection of myc tagged fragment

350 antibody. Cells were the relocated on photo-etched coverslips using recorded grid co-ordinates and expression of 6myc labelled fragments was determined by fluorescence microscopy. Data collected from cells expressing both the myc-tagged fragments (by 9E10 detection) and DsRed (determined during live cell observation) were used to make quantitative measurements of microtubule dynamic behaviour.

J. Quantification of Microtubule Dynamics

Metamorph ver. 4.0 track points function was used to track microtubule ends. Data was collected and transferred to an excel spreadsheet. Growth and shortening events were determined by eye and recorded on an excel spreadsheet. Microtubule end movements of less than 0.5 μm were not considered as growth or shortening events. Data was analysed to measure the characteristics of microtubule dynamic phases. Measurements were obtained for LLC-PK1α cells transiently expressing each of the myc-tagged MAP1a fragments and LC3 (tables III-IV). The frequency of catastrophe was determined by dividing the sum of the transitions from growth to shortening and pause to shortening by the sum of the time spent in growth and pause. The frequency of rescue was determined by dividing the sum of transitions from shortening to growth and shortening to pause by the sum of the duration of the time spent shortening by a microtubule. Dynamicity was calculated by dividing the sum of total length grown and

shortened by total time the microtubule was measured (Rusan et al., 2001). All parameters were determined for each microtubule, except for time spent in each phase, which was a cumulative total for all the microtubules measured. Statistical analysis was performed with sigma plot ver 5.0 software, using a student's t-test. For the t-test analysis, each treatment was compared to 6myc transfected LLC-PK1α cells.

Microtubule dynamics data was also used to construct life history plots for cells expressing each of the 6myc tagged MAP1a fragments and LC3. Starting from time and position zero, the displacement positions of microtubule ends were plotted at 4 second intervals. Graphs represent the migration of microtubule ends during a 2-minute period. Growth and shortening phases are represented as positive and negative slopes respectively. A positive slope followed by a negative slope represents a catastrophe event and a negative slope followed by a positive slope represents a rescue event. These graphs represent the average of all microtubules measured in each trial. Life history plots were constructed using microsoft excel.

III. RESULTS

A. Endogenous MAP expression in LLC-PK1α cells

To determine if LLC-PK1α cells expressed any of the major neuronal MAPs, whole cell extracts were separated by SDS-PAGE on 7.5% gels and blots were probed by western analysis (figure 15 A-E) using antibodies against MAP1a (HM-1), MAP1b (AA6), LC1 (E12), MAP2 (HM-2) family and Tau proteins (tau-2). All antibodies were successful in detecting each MAP in neuronal bovine brain extracts. Degredation products in bovine brain extracts were common due to the length of time between harvesting brains after animals were slaughtered and protein extraction. LC1 and MAP1b were detected in bovine brain extracts (figure 15 A, B), migrating to expected molecular weights of 330 kDa and 33 kDa respectively. MAP1a was also detected with a predicted molecular weight of 350kDa (figure 15 C). High molecular weight MAP2 (figure 15 D) was detected in bovine brain extracts along with multiple bands representing HWM MAP2 isoforms and degraded products of HMW MAP2. The Tau family consisting of several isoforms that range from 45-65 kDa, were detected in bovine brain extracts (figure 15 E). There was no evidence of endogenous expression in LLC-PK1α whole cell extracts for any of these neuronal MAPs (figure 15 A-E).

B. 6myc-tagged MAP expression in transiently transfected LLC-PK1α cells

Immunofluorescence and western analysis were used to verify the expression of myc-tagged MAP fragments in LLC-PK1α cells. All myc-tagged MAP1a (figure 16) and light chain proteins (figure 17) were detected within 10kDa of their predicted molecular weights (see figure 11 for predicted molecular weights).

Fluorescence microscopy was used to detect 6myc-tagged proteins in transiently transfected LLC-PK1α cells. All 6myc-tagged MAP1a fragments and 6myc-tagged light chains were successfully detected after cells were fixed by the precipitation fixation method. To determine if the 6myc tagged proteins were bound to microtubules, LLC-PK1α cells transfected with 6myc-tagged MAP1a fragments and 6myc-tagged light chains were fixed according to the extraction fixation protocol. Microtubules of transfected and non-transfected cells showed a normal interphase pattern. 6myc and 6mycN1a-1 (figure 18) were not detected in transfected LLC-PK1α cells after extraction fixation.

Extraction fixation of cells expressing 6mycN1a-2ΔBR showed the 6myc staining co-localized with microtubules (figure 19). Co-localization of 6myc staining with microtubule networks was also detected in cells expressing 6mycN1a-2, 6mycN1a-3, 6mycN1a-4, 6mycN1a (figure 19), 6myc LC2 and 6mycLC3 (figure 20). 6mycLC1 was detected after extraction fixation, but the 6myc staining pattern did not appear to colocalize well with microtubules (figure 20).

Expression and transfection efficiency of truncated MAP1a products decreased as the size of the truncated protein increased, with lowest levels of expression and transfection in cells expressing the full length MAP1a. LC1 and

Figure 15: Western blotting of neuronal MAPs in bovine brain extracts (bb) and whole cell protein extracts from LLC-PK1α cell s. A) LC1, B) MAP1b, C) MAP1a, D) MAP2 high molecular weight isoforms, E) Tau isoforms.

Molecular weight markers (MW) are in kDa.

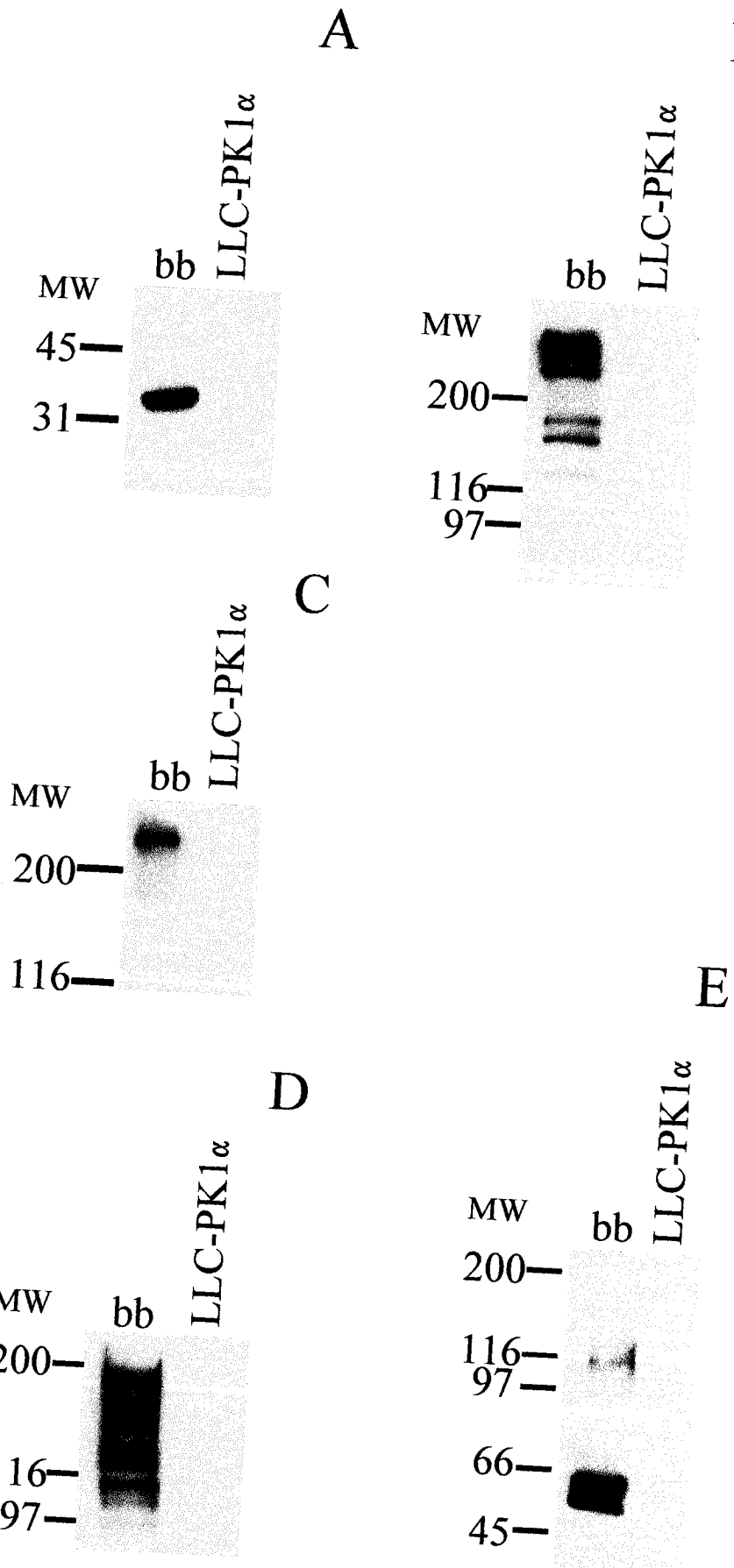
A
B
C
D
E
MW
bb
LLC-PK1α
45
31
200
116
97
66

LC2 also demonstrated relatively low expression and transfection levels in LLC-PK1α, in spite of their relatively small size.

C. Changes in detyrosinated α-tubulin

Elevated levels of detyrosinated tubulin are associated with microtubules that have increased stability and decreased turnover rates. To determine if a difference in microtubule dynamics parameters of LLC-PK1α was reflected in changes in relative amounts of detyrosinated α-tubulin, western analysis of whole cell extracts was used. Elevated levels of detyrosinated αtubulin were shown by detecting increases in optical density compared to untransfected cells in cell extracts of LLC-PK1α cells transfected with 6myc-tagged MAP fragments. 6myc N1a-2, 6mycN1a-3 and 6mycN1a-4 showed the largest increases compared to other MAP1a fragments (figure 21). 6mycLC1, 6myc LC2 and 6mycLC3 all showed large increases in detyrosinated αtubulin, even higher than MAP2c (figure 22). This suggests that light chain fragments stabilize microtubules. To ensure that similar amounts of α-tubulin were present in whole cell extracts, western blots were probed for α-tubulin using the monoclonal DM 1A Ab. LLC-PK1α cells transfected with 6mycMAP2c showed an increase in detyrosinated αtubulin compared to untransfected LLC-PK1α cells. MAP2c was used as a positive control since it has been shown to stabilize microtubules (Gamblin et al., 1996, Umeyama et al., 1993)

Figure 16: Detection of 6myc-tagged MAP1a fragments in whole cell protein extracts from transfected LLC-PK1α cells by western blotting. 33kDa, 50kDa and 66 kDa bands represent non-specific staining due to secondary antibody used in detection. * Marks the presence of each 6myc tagged fragment in whole cell extracts. Molecular weight markers (MW) are in kDa.

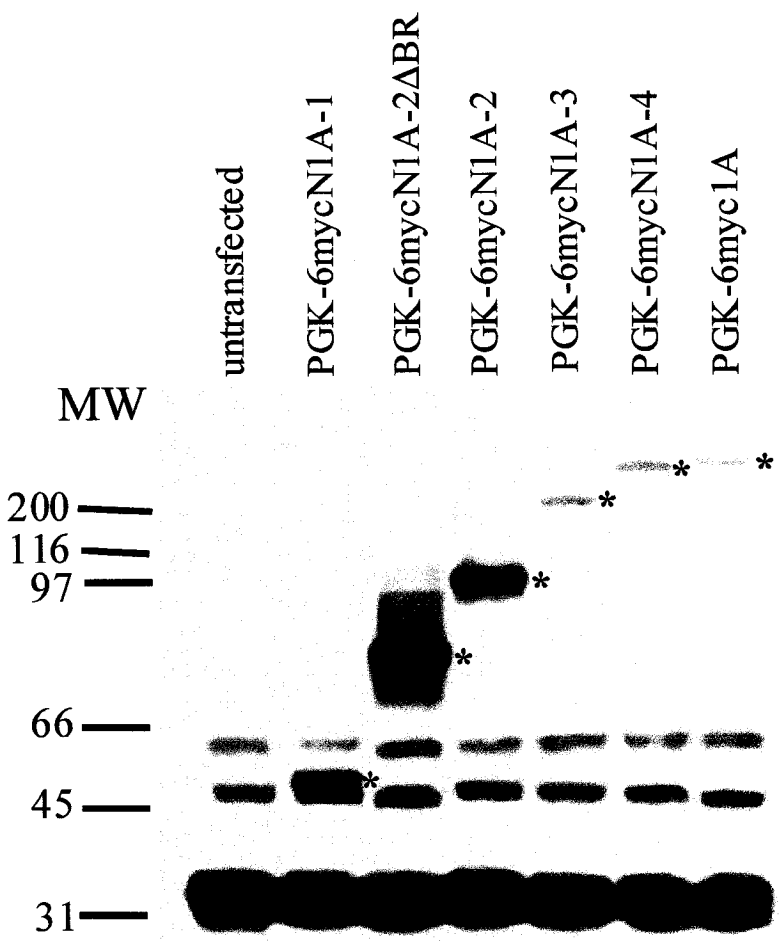
untransfected
PGK-6mycN1A-1
PGK-6mycN1A-2ΔBR
PGK-6mycN1A-2
PGK-6mycN1A-3
PGK-6mycN1A-4
PGK-6myc1A
MW
200
116
97
66
45
31

Figure 17: Detection of 6myc-tagged light chain fragments by western blotting with monoclonal 9E10 Ab in whole cell protein extracts from transfected LLC-PK1α cells. 33kDa bands represent non-specific staining due to secondary antibody used in detection. * Marks the presence of each 6myc tagged fragment in whole cell extracts. Molecular weight markers (MW) are in kDa.

LC1
untransfected
untransfected
LC2
LC3
45
31
*
*
*

Figure 18: Phase contrast images of LLC-PK1α cells after transfection with 6myc tagged fragments (a,b). Detection of GFP:αtubulin (a'-b') and 6myc tagged fragments (monoclonal Ab 9e10, a''-b'') in transfected LLC-PK1α cells by fluorescence microscopy. Both 6myc (b-b'') and 6mycN1a-1 (a-a'') were detected following precipitation fixation. Scale bar = 10μm.

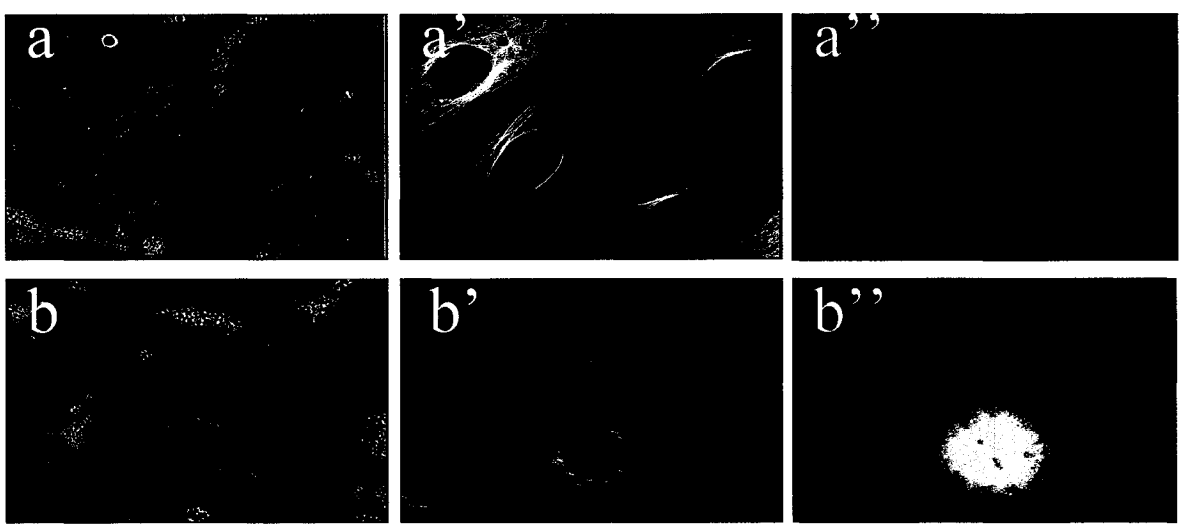
a
a'
a''
b
b'
b''

Figure 19: detection of GFP:α-tubulin (a-g) and 6myc tagged fragments (monoclonal Ab 9e10, (a'-g') in transfected LLC-PK1α cells by fluorescence microscopy. Both 6myc (a') and 6mycN1a-1 (b') were not detected following extraction fixation. 6myc N1a-2ΔBR (c'), 6mycN1a-2 (d'), 6mycN1a-3 (e'), 6mycN1a-4 (f') and 6myc1a (g') were detected after extraction fixation and colocalized continuously along microtubules (c''-g''). In overlay slides (a''-g'') green represents GFP:α-tubulin detection, red represents 6myc tag detection. Yellow signifies colocalization. Scale bar = 10μm.

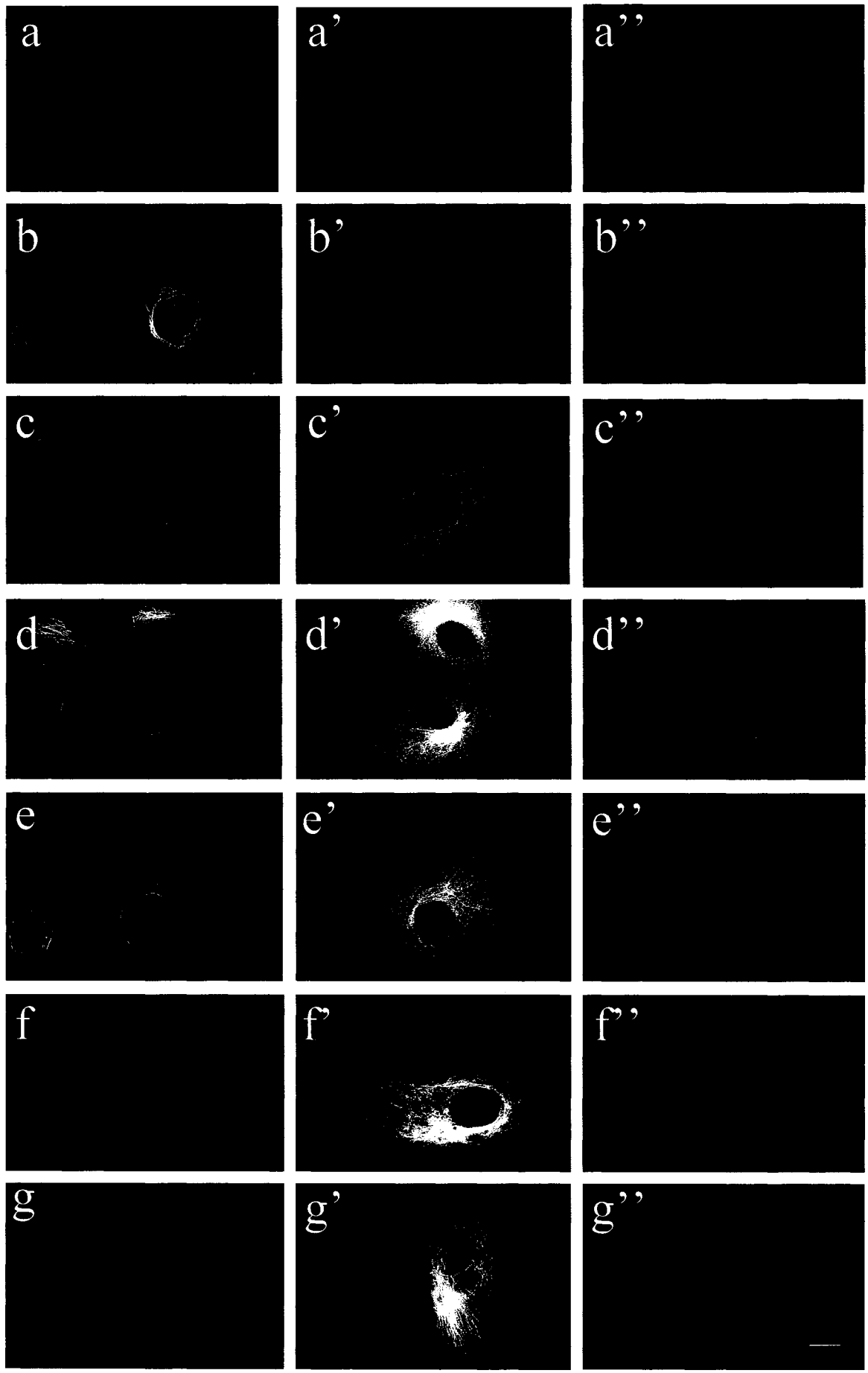
a
a'
a''
b
b'
b''
c
c'
c''
d
d'
d''
e
e'
e''
f
f'
f''
g
g'
g''

Figure 20: detection of GFP:α-tubulin (a-c) and 6myc tagged fragments (monoclonal Ab 9e10, (a'-c') in transfected LLC-PK1α cells by fluorescence microscopy. 6mycLC1(a'), 6mycLC2 (b'), 6mycLC3 (c') were detected after extraction fixation. 6mycLC1 showed very weak colocalization with microtubules (a''). Both 6mycLC2 (b'') and 6mycLC3 (c'') colocalized with microtubules after extraction fixation. In overlay slides (a''-g'') green represents GFP:α-tubulin detection, red represents 6myc tag detection. Yellow signifies colocalization. Scale bar = 10μm.

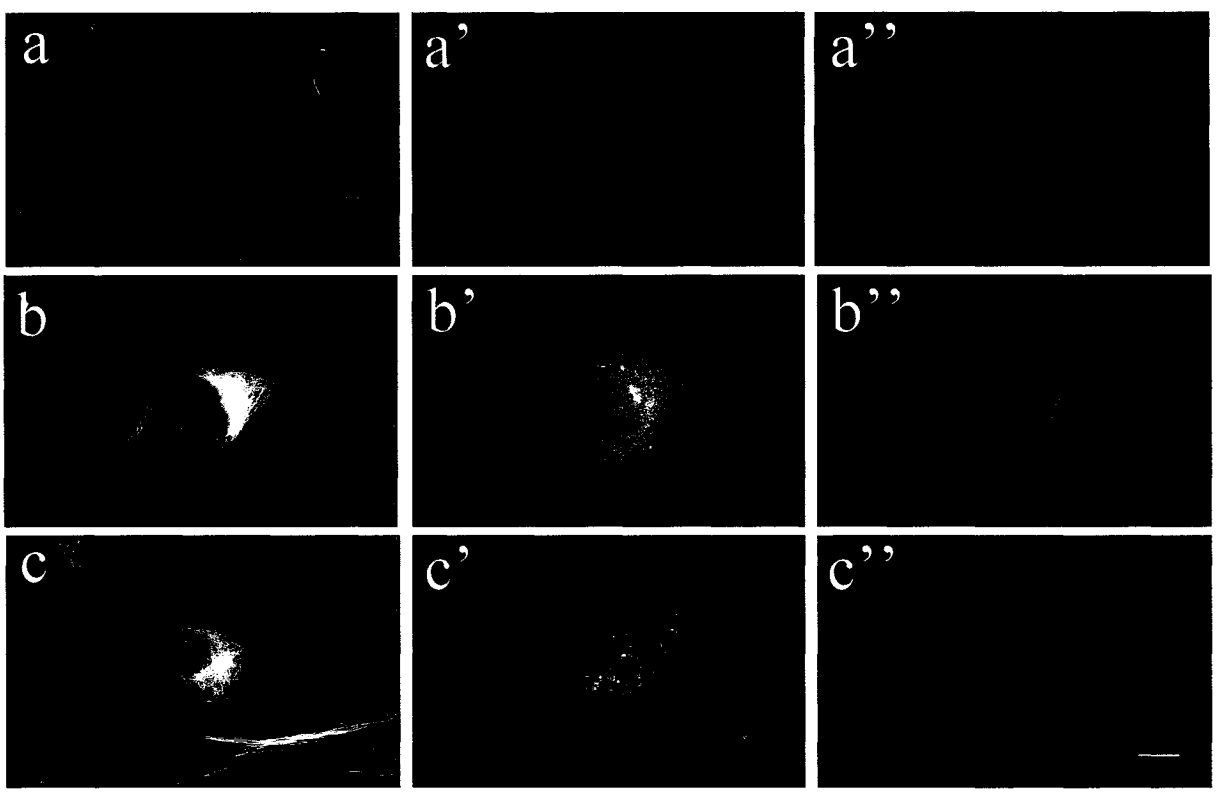
a
a'
a''
b
b'
b''
c
c'
c''

Figure 21: Detection of detyrosinated α-tubulin (A) and total tubulin (B) in whole cell protein extracts from LLC-PK1α cells expressing 6myc-tagged MAP1a fragments and 6mycMAP2c by western blotting. Numbers represent increases in the proportion of detyrosinated tubulin (measured by optical density of bands) compared to untransfected whole cell extracts.

A

untransfected
N1A-1
N1A-2ΔBR
N1A-2
N1A-3
N1A-4
1A
MAP2C
0
0.1
0.1
0.2
0.9
0.4
0.1
0.7

B

untransfected
N1A-1
N1A-2ΔBR
N1A-2
N1A-3
N1A-4
1A
MAP2C

Figure 22: Detection of detyrosinated αtubulin (A) and total tubulin (B) in whole cell protein extracts from LLC-PK1α cells expressing 6myc-tagged light chain fragments and myc-tagged MAP2c by western blotting. Numbers represent increasesin the proportion of detyrosinated tubulin (measured by the optical density of bands) compared to untransfected whole cell extracts.

A

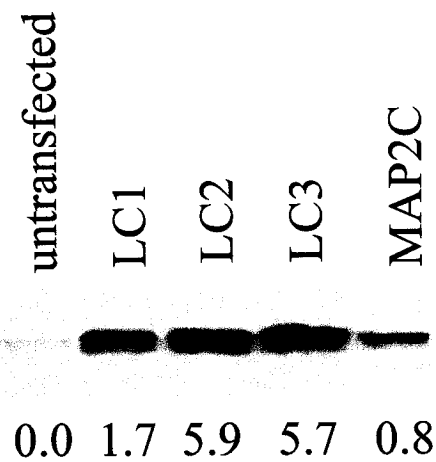
untransfected
LC1
LC2
LC3
MAP2C
0.0
1.7
5.9
5.7
0.8

B

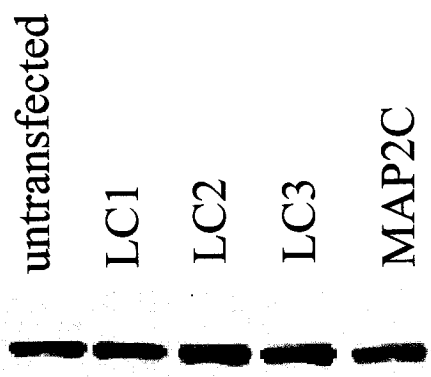
untransfected
LC1
LC2
LC3
MAP2C

D. Quantitative analysis of microtubule dynamic parameters *in vivo*

To determine the effect of 6myc-tagged MAP fragments on parameters of microtubule dynamics, interphase microtubules in transfected cells were measured by live cell fluorescence microscopy. Peripheral microtubules were clearly distinguished (figure 23) and displayed dynamic properties of alternations between growth, shortening and pause. These dynamic microtubules were suitable for performing microtubule measurements to determine changes in dynamic parameters. Individual microtubule ends were only distinguishable in the cell periphery. For this reason, dynamic events of Microtubules that emerged (or retreated) from the microtubule organizing centre rapidly could not be measured. Microtubules that remained in an attenuated state over the 2-minute period of observation were also not used.

D.1. 6myc and 6mycN1a-1

LLC-PK1α cells transfected with 6myc and 6mycN1a-1 were indistinguishable from those in untransfected LLC-PK1α cells (table III).

Figure 23: This sequence of images represents the shortening of a microtubule over a period of 24 seconds. Live LLC-PK1α cells were observed with fluorescence microscopy. Frames a-f were captured at 4 second intervals. Scale bar = 2.5 μm

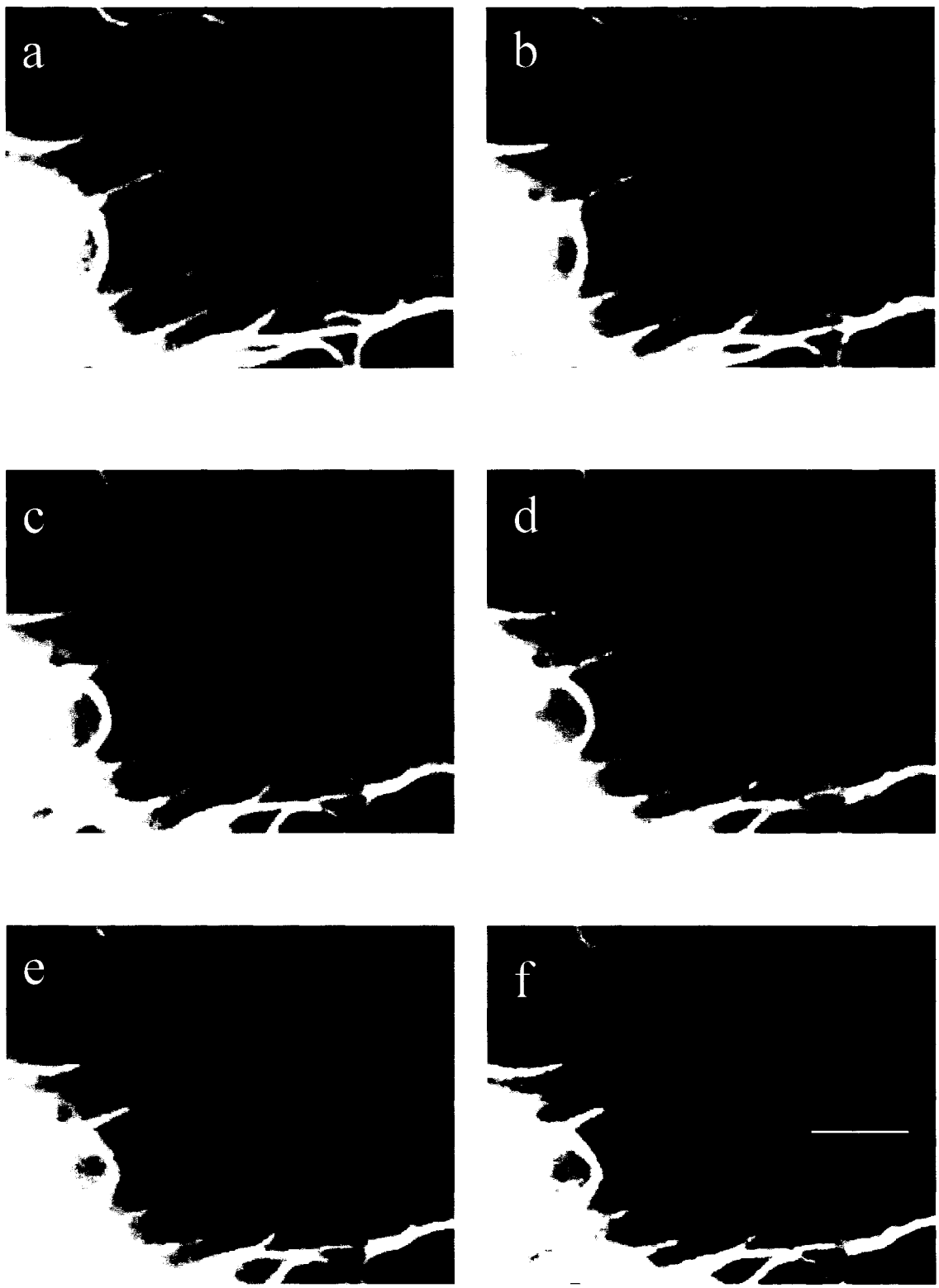
a
b
c
d
e
f

Table III: Quantification of microtubule dynamic behavior in LLC-PK1α cells expressing myc, mycN1A-1 and untransfected (control) cells

Dynamic Parameters	control	myc	mycN1A-1
Growth			
Rate (μm/min)	11.07 ± 0.36	11.38 ± 0.25	10.93 ± 0.24
Distance (μm)	1.12 ± 0.05	1.13 ± 0.04	1.02 ± 0.05
Duration (s)	5.63 ± 0.30	6.13 ± 0.18	5.97 ± 0.22
Shrink			
Rate (μm/min)	15.04 ± 0.53	15.58 ± 0.48	14.75 ± 0.54
Distance (μm)	1.80 ± 0.17	1.90 ± 0.11	1.73 ± 0.13
Duration (s)	7.25 ± 0.56	7.21 ± 0.29	6.56 ± 0.27
Pause			
Duration (s)	17.19 ± 1.65	17.14 ± 0.75	18.16 ± 1.04
% Time per phase (growth/shrink/pause)	18/14/68	17/14/69	18/14/68
Rescue frequency (events/s)	0.156 ± 0.012	0.157 ± 0.015	0.157 ± 0.009
Catastrophe frequency (events/s)	0.022 ± 0.002	0.028 ± 0.002	0.027 ± 0.002
Dynamicity (μm/min)	4.17 ± 0.20	4.43 ± 0.23	4.16 ± 0.22

* significant from myc transfected cells at a 95% confidence interval
** significant from myc transfected cells at a 99% confidence interval
statistics analyzed using a Student's t test

D.2. 6mycN1a-2ΔBR

LLC-PK1α cells expressing 6mycN1a-2ΔBR differed from 6myc transfected cells in both growth and shortening characteristics (table IV). Growth rates (10.00μm/min) decreased, but average duration of growth phases increased (7.09s) compared to LLC-PK1α cells expressing the 6myc tag (11.38μm/min, 6.13s). Shortening rate (13.15μm/min) and average distance (1.35 μm) both decreased in cells expressing 6mycN1a-2ΔBR compared to controls (15.58μm/min, 1.90μm). A decrease in microtubule dynamicity was also observed, reflecting the decrease measured in shortening phase dynamic parameters. 6mycN1a-2ΔBR expression did not appear to have a dramatic effect on overall microtubule length and microtubule stability. This was demonstrated by a relatively small increase in net microtubule length in a life history plot (figure 24) and similar levels of detyrosinated α-tubulin compared to untransfected cells (figure 22).

D.3. 6mycN1a-2

LLC-PK1α cells expressing 6mycN1a-2 also differed from 6myc transfected cells in both growth and shortening characteristics(table IV). Growth rates (9.21μm/min) and average distance lengthened (0.96μm) both decreased

Table IV: Quantification of microtubule dynamic behavior in LLC-PK1α cells expressing myc-tagged MAP1A fragments

Dynamic Parameters	myc	mycN1A-2ΔBR	mycN1a-2	mycN1A-3	mycN1A-4	myc1A
Growth						
Rate (μm/min)	11.38 ± 0.25	* 10.00 ± 0.21	** 9.21 ± 0.18	10.36 ± 0.27	* 12.13 ± 0.35	10.56± 0.31
Distance (μm)	1.13 ± 0.04	1.13 ± 0.07	* 0.96 ± 0.05	** 0.81 ± 0.04	** 1.48 ± 0.10	1.17± 0.06
Duration (s)	6.13± 0.18	* 7.09 ± 0.45	5.71 ± 0.26	** 4.64± 0.13	** 7.52 ± 0.49	6.08± 0.43
Shrink						
Rate (μm/min)	15.58 ± 0.48	* 13.15 ± 0.76	* 13.33 ± 0.73	** 10.30 ± 0.38	* 12.86 ± 0.66	**8.79 ± 0.24
Distance (μm)	1.90 ± 0.11	* 1.35 ± 0.13	* 1.43 ± 0.16	** 0.74 ± 0.04	** 1.33 ± 0.13	** 0.68 ± 0.04
Duration (s)	7.21 ± 0.29	6.37 ± 0.41	6.14 ± 0.45	** 4.25± 0.11	6.28 ± 0.52	** 4.73 ± 0.40
Pause						
Duration (s)	17.14 ± 0.75	19.88 ± 1.42	17.54 ± 0.90	* 20.01 ± 1.11	* 14.48 ± 0.87	** 26.02 ± 1.42
% Time per phase (growth/shrink/pause)	17/14/69	17/11/72	18/12/70	16/8/76	24/14/62	12/10/78
Rescue frequency (events/s)	0.157 ± 0.015	0.179 ± 0.010	0.183 ± 0.012	** 0.237 ± 0.005	0.179 ± 0.011	* 0.220 ± 0.013
Catastrophe frequency (events/s)	0.028 ± 0.002	0.021 ± 0.002	0.025 ± 0.003	0.022 ± 0.003	0.024 ± 0.002	** 0.015 ± 0.002
Dynamicity (μm/min)	4.43 ± 0.23	** 3.10 ± 0.23	** 3.00 ± 0.16	** 2.65 ± 0.20	4.80 ± 0.23	** 1.86 ± 0.24

* significant from myc transfected cells at a 95% confidence interval
** significant from myc transfected cells at a 99% confidence interval
statistics analyzed using a Student's t test

compared to cells expressing the 6myc tag(11.38μm/min, 6.13s). Shortening rate (13.33μm/min) and average distance (1.43 μm) both decreased significantly in cells expressing 6mycN1a-2 compared to cells expressing the 6myc tag (15.58μm/min, 1.90μm). A decrease in dynamicity was also observed (3.00μm/min), reflecting the decreases measured for both growth and shortening dynamic parameters. Similar to 6mycN1a-2ΔBR, 6mycN1a-2 expression did not appear to have a dramatic effect on overall microtubule length and microtubule stability. This was demonstrated by a relatively small increase in net microtubule length in a life history plot (figure 24) and similar levels of detyrosinated α-tubulin compared to untransfected cells (figure 22).

D.4. 6mycN1a-3

LLC-PK1α cells expressing 6mycN1a-3 differed from 6myc transfected cells in both growth and shortening characteristics (table IV). Growth rates were similar to 6myc expressing cells, but average distance lengthened (0.81μm) and average duration of a growth phase (4.64s) both decreased compared to cells expressing 6myc (1.13μm, 6.13s). Shortening rate (10.30μm/min), average distance (0.74 μm) and average phase duration (4.25s) all decreased dramatically in cells expressing 6mycN1a-3 compared to cells expressing the 6myc tag (15.58μm/min, 1.90μm, 7.21s) and exceeded all shortening characteristics. An increase in rescue frequency and the duration of pause phases were also determined. A decrease in dynamicity was also observed

Figure 24: Life history plots (migration of microtubule ends over a two minute period) of microtubules in LLC-PK1α cells expressing myc-taggedMAP1a fragments: 6myc (A), 6mycN1a-2ΔBR (B), 6mycN1a-2 (C), 6mycN1a-3 (D), 6mycN1a-4 (E) and 6myc1a (F). Each plot represents an average for all the microtubules measured for each fragment.

A

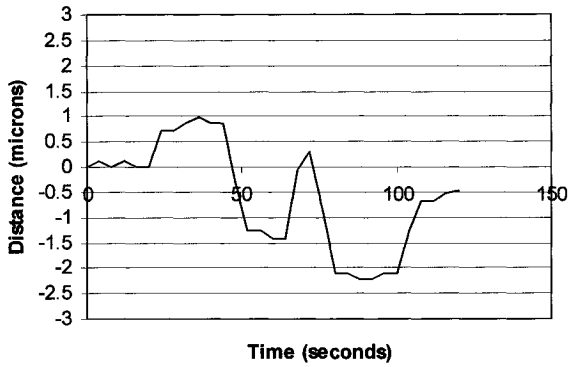
Distance (microns)
3
2.5
2
1.5
1
0.5
0
-0.5
-1
-1.5
-2
-2.5
-3
0
50
100
150
Time (seconds)

B

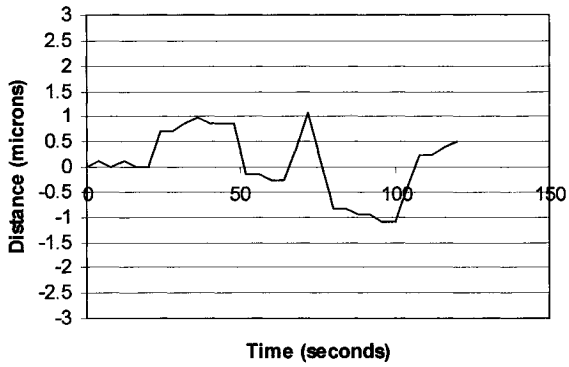
Distance (microns)
3
2.5
2
1.5
1
0.5
0
-0.5
-1
-1.5
-2
-2.5
-3
0
50
100
150
Time (seconds)

C

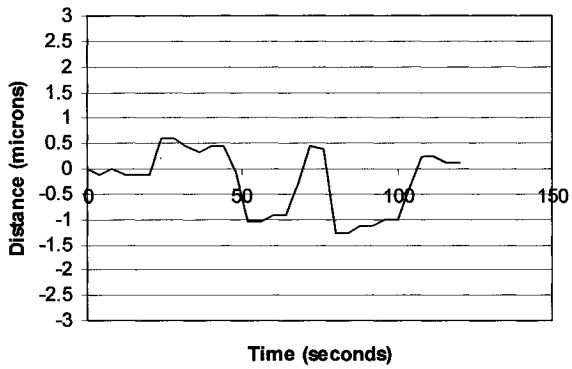
Distance (microns)
3
2.5
2
1.5
1
0.5
0
-0.5
-1
-1.5
-2
-2.5
-3
0
50
100
150
Time (seconds)

D

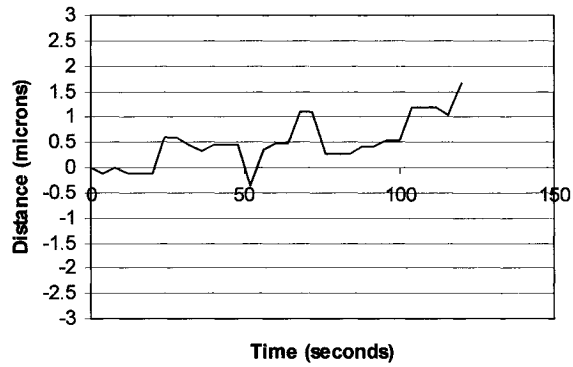
Distance (microns)
3
2.5
2
1.5
1
0.5
0
-0.5
-1
-1.5
-2
-2.5
-3
0
50
100
150
Time (seconds)

E

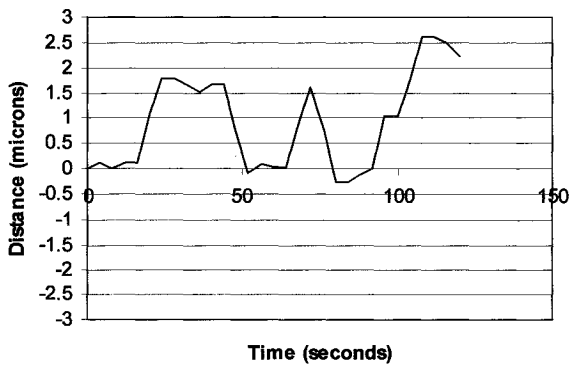
Distance (microns)
3
2.5
2
1.5
1
0.5
0
-0.5
-1
-1.5
-2
-2.5
-3
0
50
100
150
Time (seconds)

F

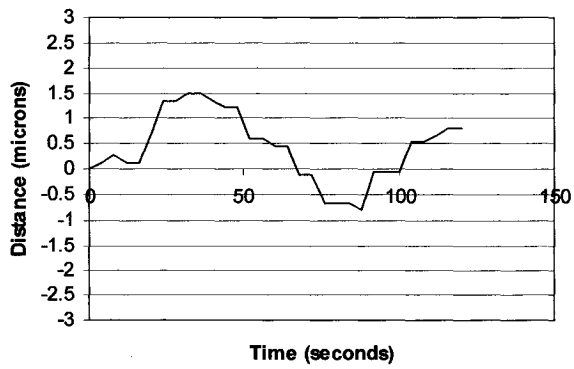
Distance (microns)
3
2.5
2
1.5
1
0.5
0
-0.5
-1
-1.5
-2
-2.5
-3
0
50
100
150
Time (seconds)

(2.65μm/min), reflecting the decreases measured for both growth and shortening dynamic parameters. Dynamic parameters of shortening were inhibited more than growth characteristics. Measured inhibitions in growth and shortening dynamic parameters appears to have a dramatic effect on microtubule dynamics. This was demonstrated by an increase in net growth in a life history plot (figure 24) and a relatively large increase of detyrosinated α-tubulin compared to untransfected cells (figure 22).

D.5. 6mycN1a-4

Growth rates (12.13 μm/min), average distance lengthened (1.48μm) and average duration of a growth phase (7.52s) all increased in LLC-PK1α cells expressing 6mycN1a-4 compared to cells expressing the 6myc tag (11.38μm/min, 1.13μm, 6.13s). Shortening rate (12.86μm/min) and average distance (1.33 μm) decreased in cells expressing 6mycN1a-4 compared to cells expressing the 6myc tag (15.58μm/min, 1.90μm). Dynamicity of microtubule populations was similar to untransfected cells. This reflects inhibition of shortening parameters being offset by an increase in growth event characteristics. Measured inhibitions in growth and shortening dynamic parameters appears to have dramatic effects on microtubule dynamics. This was demonstrated by an increase in net growth in a life history plot (figure 24) and a relatively large increase of detyrosinated α-tubulin compared to untransfected cells (figure 22).

D.6. 6myc1a

Growth characteristics were similar in LLC-PK1α cells expressing 6myc1a compared to cells expressing the 6myc tag (table IV) . A relatively large decrease was measured in shortening rate (8.79μm/min), average distance (0.68 μm) and average shortening duration (4.73s) compared to cells expressing the 6myc tag (15.58μm/min, 1.90μm, 7.21s). Dynamicity of microtubule populations was found to decrease dramatically (1.86μm/min) to the lowest level measured in all microtubules. This reflects a significant inhibition of shortening dynamic parameters. Cells expressing 6myc1a also demonstrated an increase in rescue and a decrease in catastrophe frequency. Average pause phase duration was also increased (26.02s) compared to cells expressing 6myc (17.14s). Measured inhibitions in growth and shortening dynamic parameters appears to have dramatic effect on microtubule dynamics as demonstrated by an increase in net growth in a life history plot (figure 24). A significant difference was not detected in detyrosinated αtubulin compared to untransfected cells (figure 22). This is most likely due to the relatively low transfection efficiencies of 6myc1a (below 1%) in whole cell extracts.

D.7. 6mycLC1 and 6mycLC2

Live cell data was not obtained from cells expressing either of these proteins. Even though levels of α-tubulin detyrosination were considerably higher in LLC-PK1α cells expressing these light chain molecules, the extremely low expression did not allow detection of 6myc tags by immunofluorescence staining with the alexa 350 antibody. This made it impossible to identify the transfected cells by microscopy.

D.8. 6mycLC3

Growth characteristics of microtubules were inhibited to a relatively small degree in cells expressing 6mycLC3 (Table V). Microtubules showed a decrease in rate (9.68 μm/min), distance (0.81μm) and duration of a growth phases (5.08s) compared to cells expressing the 6myc tag (11.38μm/min, 1.13μm, 6.13s). A relatively large decrease was measured in shortening rate (10.08μm/min), average distance (0.88 μm) and average shortening duration (4.99s) compared to cells expressing 6myc (15.58μm/min, 1.90μm, 7.21s). Dynamicity of microtubule populations was found to decrease significantly (2.19μm/min). Most of this change in dynamicity reflects the inhibition of shortening dynamic parameters. Cells expressing 6mycLC3 also demonstrated an increase in rescue and a decrease in catastrophe frequency (table V). Average pause phase duration was also increased (23.46s) compared to cells

Table V: Quantification of microtubule dynamic behavior in LLC-PK1α cells expressing myc and myc-tagged light chain 3.

Dynamic Parameters	myc	mycLC3
Growth		
Rate (μm/min)	11.38 ± 0.25	** 9.68 ± 0.19
Distance (μm)	1.13 ± 0.04	** 0.81 ± 0.03
Duration (s)	6.13 ± 0.18	** 5.08 ± 0.16
Shrink		
Rate (μm/min)	15.58 ± 0.48	** 10.08 ± 0.36
Distance (μm)	1.90 ± 0.11	** 0.88 ± 0.06
Duration (s)	7.21 ± 0.29	** 4.99 ± 0.23
Pause		
Duration (s)	17.14 ± 0.75	** 23.46 ± 1.41
% Time per phase (growth/shrink/pause)	17/14/69	14/9/77
Rescue frequency (events/s)	0.157 ± 0.015	** 0.212 ± 0.008
Catastrophe frequency (events/s)	0.028 ± 0.002	** 0.019 ± 0.002
Dynamicity (μm/min)	4.43 ± 0.23	** 2.19 ± 0.13

* significant from myc transfected cells at a 95% confidence interval
** significant from myc transfected cells at a 99% confidence interval
statistics analyzed using a Student's t test

Figure 25: Life history plots (migration of microtubule ends over a two minute period) of microtubules in LLC-PK1α cells expressing myc (A) and myc-tagged light chain3 (B). Each plot represents an average for all the microtubules measured for each fragment.

A

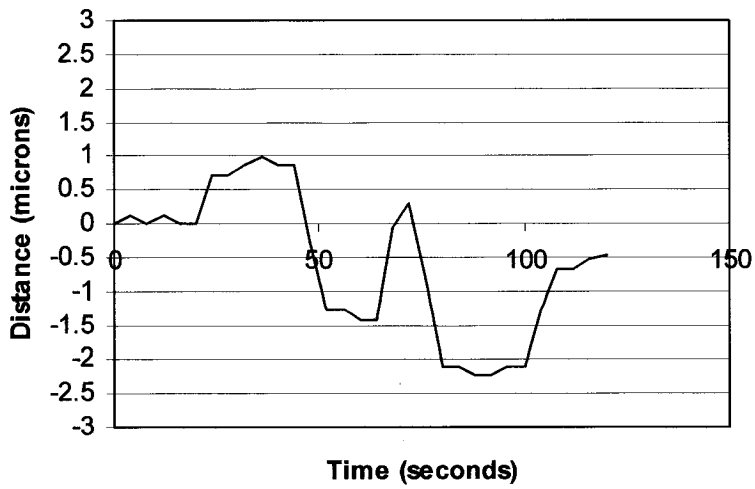
3
2.5
2
1.5
1
0.5
0
-0.5
-1
-1.5
-2
-2.5
-3
0
50
100
150
Distance (microns)
Time (seconds)

B

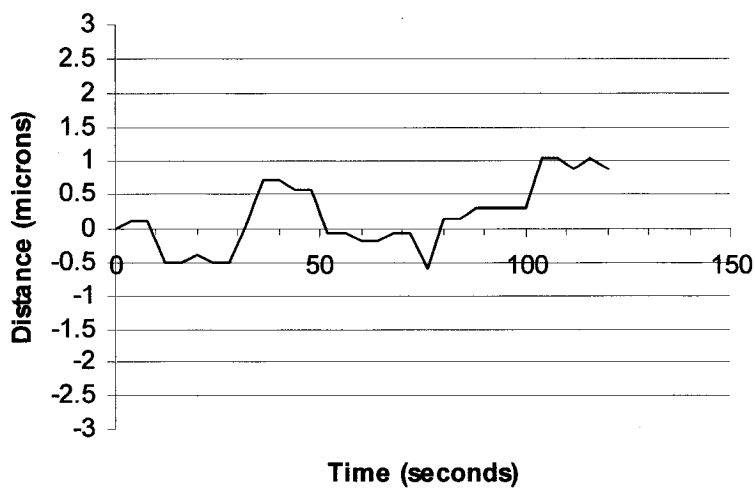
3
2.5
2
1.5
1
0.5
0
-0.5
-1
-1.5
-2
-2.5
-3
0
50
100
150
Distance (microns)
Time (seconds)

expressing the 6myc tag (17.14s). Expression of 6mycLC3 appears to have a dramatic effect on microtubule dynamics as demonstrated by an increase in net growth in a life history plot (figure 25) and relative increase in detyrosinated α-tubulin compared to untransfected cells (figure 23).

D.9. 6myc MAP2c

Peripheral microtubule ends of LLC-PK1α cells expressing 6mycMAP2C did not appear to undergo phases of growth and shortening and individual and MAP2c-bundled microtubules remained in an attenuated state over the 2-minute periods of observation (figure 26). Cells expressing 6mycMAP2c were significantly smaller than untransfected and 6myc-tagged MAP fragment expressing cells. 6mycMAP2c expressing cells were often half of the diameter of other LLC-PK1α cells.

Figure 26: Live LLC-PK1α cells transiently transfected with 6mycMAP2c were observed using fluorescence microscopy over a period of 96 seconds. Frames a-i were captured at 12 second intervals. Scale bar = 5 μm

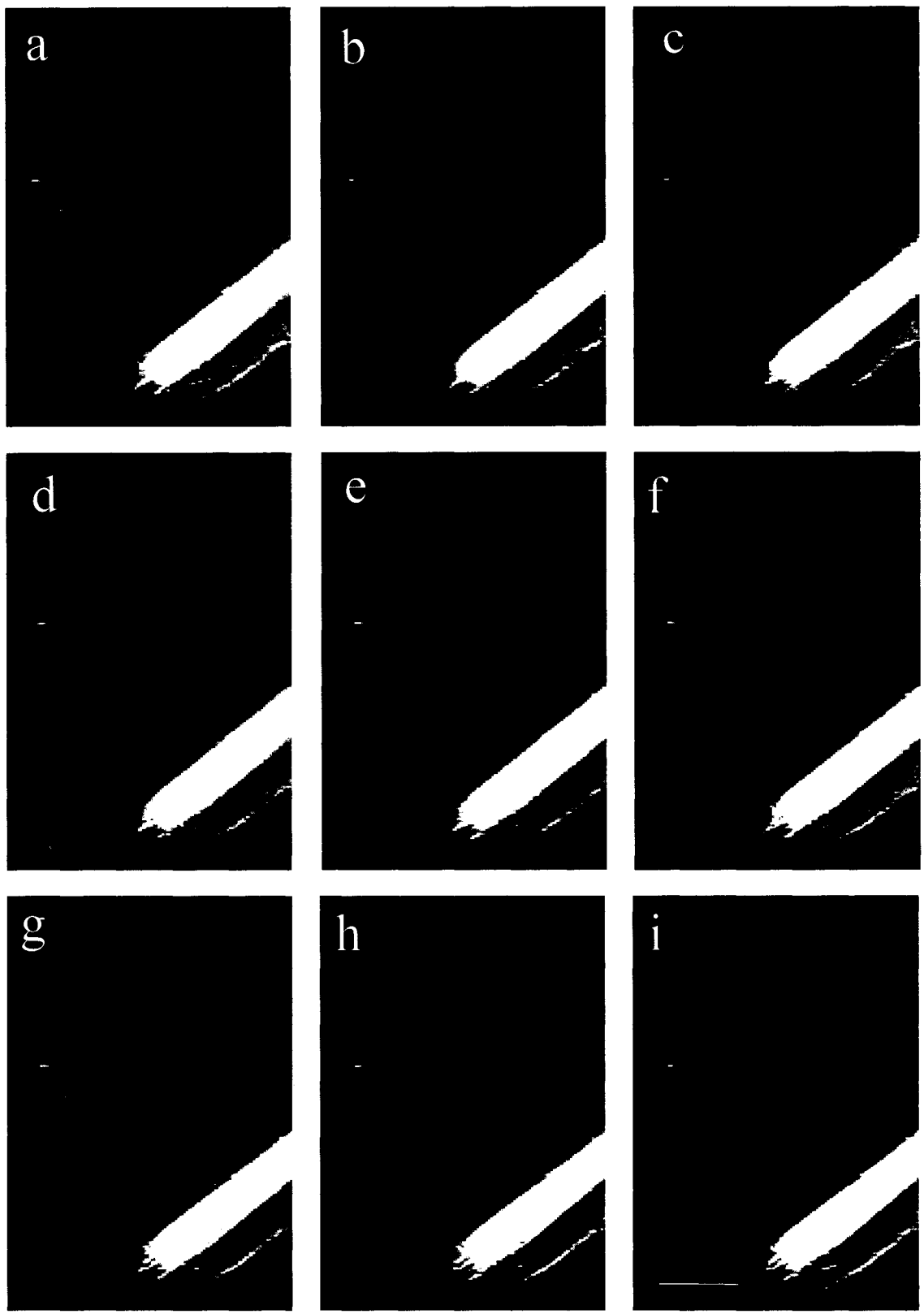
a
b
c
d
e
f
g
h
i

IV. DISCUSSION

A. Interference of Endogenous MAPs

A wide range of MAPs have been shown to modulate microtubule dynamics by increasing the stability and promoting growth of microtubules (Chapin and Bulinski, 1992; Weisshaar et al., 1992; Weisshaar and Matus, 1993; Olson et al., 1995; Pedrotti and Islam, 1995; Trinczek et al., 1995; Gamblin et al., 1996; Kalcheva et al., 1998.) Using the available antibodies for neuronal MAPs it was determined by western analysis that LLC-PK1α cells do not express detectable levels of tau, MAP2, LC1, MAP1b and MAP1a. LLC-PK1α is a porcine kidney derived cell line. Results from this study support previous findings that MAP1a is not expressed in kidney tissue (Mann and Hammarback, 1994; Fink et al., 1996). The absence of tau, MAP2, LC1 and MAP1b was also expected. These MAPs are predominantly expressed in neurons (Bloom et al., 1984; Dotti et al., 1987; Tucker et al., 1988). They are rarely found in non-neuronal tissues. It is reasonable to assume that these MAPs do not modulate microtubule dynamics in LLC-PK1α cells. MAP4 is found in many cell lines and tissues including kidney (Chapin et al., 1995). MAP4 has been shown to increase the rate of microtubule polymerization and stabilize microtubules against drug induced depolymerization (Aizawa et al., 1991; Olson et al., 1995). It is possible that MAP4 was expressed in the LLC-PK1α cell line used in this study and this may have some effect on the magnitude of effects of the MAP fragments transfected in the present study.

B. Interference of GFP

GFP has been used to tag a wide range of cytoskeletal proteins without altering protein behaviour (Ludin et al., 1996; Ludin and Matus, 1998). α-tubulin-GFP expression in LLC-PK1α cells did not interfere with the ability of LC3 and MAP1a molecules to bind microtubules. However, the GFP tag may have interfered with LC1-microtubule interaction. LC1 and LC2 have been shown to organize microtubules of HeLa and PtK2 cells into wavy bundles that are associated with increased stability against microtubule depolymerizing drugs (Togel et al., 1998; Ungureanu, 2002; Villeneuve, 2003). LC1 and LC2 expression did not appear to alter the organization of microtubules in LLC-PK1α cells used in this study. Again, the α-tubulin GFP tag may be responsible for the failure of these light chain molecules to bundle microtubules in LLC-PK1α cells.

C. MAP1a Fragments Vary in Their Ability to Alter Microtubule Dynamics

Although the number of microtubules measured in each trial varied from 20-50, the amount of standard error for each parameter remained relatively constant. This suggests that individual microtubules were being affected by their interaction with MAP fragments and the effect was relatively consistent from cell to cell and between individual microtubules. It is also important to note that these results represent the impact of MAP1a in the peripheral regions of the cell and may not reflect microtubule dynamics events in regions closer to the centrosome.

The peripheral regions of cells are the best areas to observe microtubule dynamics *in vivo* because microtubule ends are easily distinguishable.

Microtubules in untransfected LLC-PK1α cells went through the various phases of growth, shortening and pause. The measurements of microtubule dynamics performed in this study agree with previous measurements of dynamic events in LLC-PK1α cells with respect to growth shortening, pause, rescue, catastrophe and dynamicity of peripheral interphase microtubules (Rusan et al., 2001).

MAPs exert their effect on microtubules by binding to them. Both the 6myc tag and N1a-1 were not expected to have an impact on microtubule dynamics because they lack the repeat and flanking regions that have been reported to be responsible for binding MAP1a to microtubules (Vaillant et al., 1998). More recently, Villeneuve (2003) has shown weak binding of the N1a-1 fragment to microtubules *in vitro*, but did not detect binding *in vivo*. Consistent with these studies, neither fragment altered the parameters of microtubule dynamics.

The 6mycN1a-2ΔBR fragment contains the amino terminus end ligated to the regions that flank the repeat region of MAP1a and has been shown to bind to microtubules (Vaillant, 1998). Although expression of this fragment had a measured effect on microtubule dynamics there was no net effect on overall lengthening and no detectable increase in detyrosinated tubulin. This was due to the fact that an increase in the duration of lengthening events was countered by an equivalent decrease in shortening.

The 6mycN1a-2 fragment contains the amino terminus including the repeat and flanking regions of MAP1a. The effect of N1a-2 microtubule binding had a relatively small positive effect on net microtubule growth. This increased stability was also detected as a relatively small increase in α-tubulin detyrosination in whole cell extracts. This suggests that the combined flanking and repeat regions of MAP1a have a greater effect on microtubule dynamics than the flanking regions alone.

The 6mycN1a-3 fragment contains the amino terminus of MAP1a including the repeat and flanking regions and a portion of the MAP1a projection domain. The N1a-3 fragment inhibited shortening to a larger degree than all other fragments except full length MAP1a.

The N1a-4 region contains the same regions as N1a-3 with an additional portion of the projection domain. The N1a-4 region was the only fragment that had a positive impact on growth events. Although this region appears to promote growth, N1a-4 did not appear to alter the transition frequencies of catastrophe and rescue. The fainter band resulting from immunostaining for detryosinated αtubulin can be attributed to the low transfection efficiency (2%) of this relatively large fragment. Vaillant et al., (1998) detected a decrease in detyrosinated tubulin in P19 EC cells expressing the N1a-4 fragment. Elevated levels of detyrosinated tubulin and microtubule stability are not directly related (Khawaja et al., 1988). Relative levels of acetylated and detyrosinated tubulin have been shown to vary depending on the cell line (Pimperno et al., 1987; Schulze et al., 1987; Bulinski et al., 1988). These changes are attributed to differences in the

activity of the enzymes that modify tubulin. This may be the reason that detyrosinated tubulin levels in the present study do not agree with the findings of Vaillant et al., (1998).

6myc1a contains the entire MAP1a protein including LC2. Inhibition of shortening alterations in transition frequencies and increased duration of pause resulted in the largest decrease in dynamicity compared to other MAP1a fragments. However, the measured increase in stability was not associated with a detectable increase in detyrosinated α-tubulin in whole cell extracts. This can again be attributed to the extremely low transfection efficiency (below 1%) achieved in this study, due to the large size of the full length MAP1a protein. Vaillant et al., (1998) showed that only the 6myc1a gave increased levels of detyrosination. It is also important to note that the full length MAP1a construct used in this study includes the LC2 sequence. It is possible that the measured effect of the full length MAP1a may represent (at least in part) the impact of LC2 on microtubules.

The truncated versions of MAP1a in this study containing the projection domain had an effect on microtubule dynamics that was often similar to full length MAP1a. All MAP1a fragments (except N1a-4) that bound to microtubules induced a decrease in microtubule dynamicity that varied for each individual fragment. This suggests that MAP1a binding can suppress dynamic instability. MAP1a fragments containing the projection domain all increased the net growth of microtubules. MAP1a induced Increases in microtubules growth would result in increasing the size of the GTP cap. A longer GTP cap would resist

depolymerization and would contribute to the increased stability of MAP1a bound microtubules in this study.

MAP1a fragments that showed a relatively large inhibition of shortening events (N1a-3, 1a) also altered transition frequencies and had the largest impact on dynamicity. This suggests that suppression of the shortening phase is important to increase microtubule stability. Interphase microtubules undergo periods of rapid shortening and slower growth. Cells expressing N1a-3, N1a-4 and full length MAP1a had shortening phase parameters that were similar to growth phases. In some cases growth phase parameters were greater than shortening events.

D. The Projection Domain Regulates MAP1a Function

The amino end of the MAP1a protein containing the repeat and flanking regions were confirmed in this study as being responsible for binding to microtubules. The amino portion of MAP1a preceding these repeat and flanking regions did not appear to have an impact on microtubule dynamics and may be involved in associating with its light chain molecules (Kuznetsov et al., 1986; Schoenfeld et al., 1989; Muller et al., 1994; Mann and Hammarback, 1994). However, Villeneuve (2003) reported that light chain 2 does not associate with the N1a-1 region when it is expressed in HeLa cells *in vivo*.

Results from this study suggest that the projection domain of MAP1a determine its functional properties *in vivo*. This finding is supported by other

studies on the impact of different MAPs on microtubule dynamics. The GFP tagged MAP4 projection domain appears to regulate the interaction of the MAP4 microtubule-binding domain with microtubules (Olson et al., 1995). Specific regions of the MAP4 projection domain are responsible for inducing stability against depolymerization by nocodazole.

The projection domains of MAP2 proteins have been shown to be responsible for its ability to promote growth and microtubule stability. Specific regions of tau's carboxy terminus protect microtubules against disassembly and catastrophic events (Trinczek at al., 1995). These areas have been referred to as activity "hot spots". In this study the carboxy projection domain of MAP1a was also responsible for promoting microtubule growth and stability. MAP1a fragments containing the projection domain (N1a-3, N1a-4 and 1a) varied in their ability to promote microtubule growth and stability (figure 27). This suggests that these regions may contain separate activity hot spots. In the present study, these activity hot spots were expressed with neighboring regions of MAP1a. The N1a-3, N1a-4 and 1a regions may require the presence of neighboring projection domain regions to exert their effect on microtubule dynamics. Synthetic peptide sequences containing only assembly promoting regions of MAP4 have been shown to promote microtubule growth less effectively than the MAP4 entire protein (reviewed by MacRae, 1992).

The phosphorylation state of MAPs has been shown to alter their ability to bind and stabilize microtubules (Trinczek et al., 1995, Gong et al., 2000). MAP1b has been shown to exist in 2 phosphorylation states which appear to modify

Figure 27: Different regions of MAP1a and their effects on microtubule dynamic parameters. Cells expressing MAP1a fragments showed an (+) increase, (-) decrease or no change (nc) in microtubule dynamic parameters depending on the fragment.

MAP1a Fragment	Microtubule Dynamic Event					
	growth	shortening	pause	catastrophe	rescue	dynamicity
N1a-1 	nc	nc	nc	nc	nc	nc
N1a-2ΔBR 	−	−	nc	nc	nc	−
N1a-2 	−	−	nc	nc	nc	−
N1a-3 	−	− −	+	nc	+	−
N1a-4 	+	−	−	nc	nc	nc
1a 	nc	− − −	+ +	−	+	− −

the action of MAP1b *in vivo* (Ramon-Cuento and Avila, 1999). The growth promoting and shrink inhibiting domains discovered in MAP1a may also be regulated by phosphorylation.

E. Effect of MAP2c on Microtubule Dynamics

MAP2c was intended as a positive control due to its ability to stabilize microtubules (Takemura et al., 1992; Umeyama et al., 1993; Gamblin et al., 1996). In this study, transient expression of MAP2c resulted in a complete suppression of microtubule dynamics in LLC-PK1α cells. Bundled and individual microtubules did not change in length over the entire observation duration of 2 minutes. Increases in microtubule bundle length in cells expressing MAP2c have been shown over longer time periods of 120 min (Umeyama et al., 1993). One explanation for not detecting a change in microtubule growth in cells expressing MAP2c in this study could be that dynamic events were suppressed to a point where changes could not be detected over the 2-minute observation. Another explanation could be that expression levels of MAP2c were high enough to completely suppress dynamic instability *in vivo.* High concentrations of MAP2c have been shown to suppress dynamic instability *in vitro* to a point where no catastrophes or dynamic events occurred during 84 minutes of observation (Umeyama et al., 1993, Gamblin et al., 1996). In the present study transient transfection of MAP2c did give a significantly higher expression and transfection efficiency compared to any of the MAP1a fragments.

Expression of MAP2c resulted in an increase of detyrosinated tubulin detected in whole cell extracts. Vaillant et al., (1998) showed that detyrosination levels in P19 EC cells were 2 times greater compared to cells expressing MAP1a. Our results suggest that some of the MAP1a fragments increased tubulin detyrosination more than MAP2c. However, detyrosinated tubulin levels vary depending on the cell line. Takemura et al., (1992) did not detect elevated levels of detyrosinated tubulin in COS cells expressing MAP2c. They suggested that MAP2c might interfere with the binding of the detyrosinated tubulin antibody.

In contrast to the fore mentioned effects of MAP2c on microtubule dynamics found in this study, Kaech et al., (1996) reported that MAP2c and tau constructs labeled with GFP do not change the rates of microtubule growth and shrinkage *in vivo*. The effect of MAP2c on microtubule dynamics diminishes as the amount of MAP2c present diminishes (Gamblin et al., 1996). A lower expression level of MAP2c could be the reason that MAP2c expression did not alter growth and shrinking rates in their study (Kaech et al., 1996). The present study used a combination of

liposome transfection and expression booster reagents that could have resulted in a higher level of expression than the calcium phosphate coprecipitation procedure used by Kaech et al., (1996). They also neglected to report complete data on microtubule dynamic events in cells expressing MAP2c and tau. Values for rates transitions (catastrophe and rescue), dynamicity, pause, growth (distance and duration) and shortening (distance and duration) were not reported. They also neglected to provide data on the percentage of time

microtubules spent in phases of growth, shortening and pause. This makes it difficult to draw any conclusions about the effect of MAP2c on microtubule dynamics from their study. The fact that they observed "hundreds of cells" (the present study uses 3-5 cells per fragment) suggests that the events of growth and shortening they observed were relatively rare. Rates of growth and shortening may not be altered but the frequency and duration of these events appears to be suppressed dramatically in cells expressing MAP2c in the present study and previously by Umeyama et al., (1993) and Gamblin et al., (1996).

F. Effect of LC3 on Microtubule Dynamics

LC3 expression resulted in the suppression of dynamic instability reflected in all the parameters measured. An increase in microtubule stability was shown by an increase in net microtubule length and increased levels of detyrosinated tubulin compared to untransfected cells. The effect of LC3 on microtubule dynamics was similar to full length MAP1a, but MAP1a expression failed to result in an increase in tubulin detyrosination. This is attributed to the extremely low transfection efficiency of MAP1a (below 1%) compared to LC3 (18%).

LC1 and LC2 have been shown to bind microtubules and induce the formation of wavy microtubule bundles that are able to resist drug-induced depolymerization. Similar to MAP1a, LC3 expression failed to increase the ability of microtubules to resist depolymerization and did not bundle microtubules (Villeneuve, 2003).

Very little is known about the role of LC3. Results from this study demonstrate that LC3 can have a significant impact on microtubule dynamics. LC3 promotes growth and stabilizes microtubules *in vivo*. The effect of LC3 was similar to the effect that MAP1a had on microtubule dynamics. This suggests that LC3 may have a similar role to MAP1a. Since light chains are almost always expressed in locations which also express heavy chain molecules, future experiments should seek to discover the effect that light chains have in the presence of their heavy chain molecules. Evidence suggests that the presence of MAP1a can alter the ability of LC2 molecules to bundle microtubules (Villeneuve, 2003). MAP1a can bind to LC3 but this interaction *in vivo* has not been examined.

G. Role of MAP1a *in vivo*

MAP1a is the predominant MAP in the adult brain, but one of the least understood of the neuronal MAPs. Mature neuronal microtubules are characterized by increased microtubule stability against depolymerizing drugs. Since MAP1a reaches its peak expression in mature neurons, it would seem likely that MAP1a has a role in increasing the stability of microtubules. MAP1a has demonstrated inconsistent and varying abilities to stabilize microtubules. Elevated levels of detyrosinated tubulin are associated with decreased microtubule turnover and increased stability against microtubule depolymerizing drugs (reviewed in Falconer et al., 1994). N1a-2, N1a-3, N1a-4 and LC3

expression resulted in an increase of detyrosination of microtubules, but they did not appear to stabilize microtubules against depolymerization with nocodazole (Villeneuve, 2003). The fact that MAP1a and LC3 bound microtubules are not resistant to nocodazole, may be because MAP1a and LC3 do not induce microtubule bundling. MAP proteins that bundle microtubules have demonstrated stabilization of microtubules against depolymerizing drugs. The decreased dynamicity observed for all fragments suggests that MAP1a promotes a limited stability to microtubules, but still increases the net growth of microtubules through a greater inhibition of shortening compared to growth. While this stability may be important *in vivo*, it appears to have little to no protection against drug induced depolymerization.

A causal relationship between the high expression levels of MAP1a and increased microtubule stability in neurons may be an oversimplification of the function of MAP1a. This study provides evidence that MAP1a is a weak stabilizer of microtubules that promotes microtubule growth *in vivo*. MAP1a accumulates in periods of development characterized by neuronal growth, and is expressed in locations of the brain where growth persists. The presence of MAP1a in the developing spinal cord suggests MAP1a is important in neurogenesis (Oudega et al., 1998). MAP1a has been detected at high levels in both mature and developing dendritic processes where growth persists (Schoenfeld et al., 1989). MAP1a detection varies from axon to axon and was associated with areas of the brain active in growth (Bloom et al., 1984). These studies suggest that any increased stability of axonal microtubules is not because of MAP1a.

Approximately half of the microtubules of an axon appear to be in a labile state (Nixon, 1988). Individual microtubules in the axon have been found contain similar amounts of labile and stable regions throughout the axon (Baas and Black, 1990). Distal regions of axons contain the most labile microtubules. MAP1a is expressed throughout the neuron, but is concentrated in dendrites. In mature dendrites, plasticity and restructuring are important in maintenance and proper functioning of mature neurons (Keach et al., 2001).

Neuronal microtubules need to be stable, but must also be able to accommodate changes and allow for remodeling of mature neurons. MAP1a may play a role in dendrite maintenance and restructuring which requires limited microtubule plasticity, not rapid and extensive growth during embryonic development. Additional evidence that suggests a more dynamic role for MAP1a is the observation that regenerating sciatic neuronal axons display adult patterns of MAP expression, maintaining high levels of MAP1a (Fawcett et al., 1994).

Transgenic studies provide co-relational evidence that MAP1a promotes growth and stabilizes microtubules. The nervous system of tau deficient mice appears to be normal immunohistologically, with few neuronal defects. Suprisingly, these tau deficient animals were viable and axonal elongation was not affected in cultured neurons from these animals. Interestingly, MAP1a was shown to increase in the cerebrum of these tau deficient animals (Harada et al., 1994). Microinjection of tau *In vivo*, has shown that tau functions primarily to promote tubulin polymerization, decrease the depolymerization rate and stabilize microtubules (Drubin and Kischner, 1986). MAP1a up regulation may be

responsible for the viability of these tau knockout mice, suggesting that MAP1a can promote growth and stabilize microtubules to compensate for the absence of tau.

H. Importance of MAP1a Late in Neuronal Development

The fact that MAP1a causes a small increase in microtubule stability (compared to MAP2) and small promotion of growth (compared to MAP1b) may be developmentally important. These microtubule dynamic characteristics in the presence of MAP1a may be required for maintenance and remodeling of microtubules at maturity. The slow, stable nature of microtubule growth has been demonstrated *in vitro*. Microtubules polymerized *in vitro* in the presence of MAP1a are short and straight, compared to those polymerized with MAP1b which are long and bendy (Pedrotti et al., 1996b). Increased rigidity of microtubules has been associated with increased stability (Mickey and Howard, 1995).

MAP1a is also capable of interacting with all 3 light chains (MAP1b only associates with 2). Heavy chains may modify the actions of light chain fragments, making MAP1a more versatile than MAP1b in this respect. The ability to interact and regulate the actions of all 3 light chain molecules may be important in mature neurons.

Levels of MAP1a increase with neuronal development and MAP1b decreases (Oblinger and Kost, 1994). MAP2 and MAP1b compete for binding sites on microtubules (Pedrotti and Islam, 1995). MAP1a and MAP2 can bind on same

microtubule and may interact to have a cooperative effect on microtubule dynamics (Shiomura and Hirokawa, 1987). MAP2 proteins have been shown to stabilize microtubules and resist drug-induced depolymerization. As neurons develop, an increase in MAP1a expression (and decrease in MAP1b) may increase the stability of neurons against depolymerization indirectly by allowing increasing amounts of MAP2 to associate with microtubules.

The number of glutamyl residues attached to β-tubulin increases with development (Redeker et al., 1996). Adult forms of highly polygluatmylated tubulin show increased affinity for MAP1a compared to MAP2, tau and MAP1b (Audebert et al., 1994; Boucher et al., 1994; Bonnet et al., 2001). The ability of MAP2, tau and MAP1b to bind tubulin decreases as the length of the glutamyl chain on β-tubulin increases. This suggests that MAP1a has a greater affinity than other adult MAPs to microtubules that are predominant late in development. The ability of MAP1a to efficiently bind highly glutamylated microtubules suggests that MAP1a is well suited to stabilize microtubules late in development.

I. Concluding Remarks

This study shows that MAP1a and LC3 have a direct impact on microtubule dynamics *in vivo*. In this study the ability of MAP1a to stabilize microtubules was lower than MAP2c. Embryonic stages of growth are chacterized by the rapid growth and development of immature neurons. Maturity requires the presence of a protein that is capable of growth and remodeling in a stable and relatively slow manner compared to the rapid embryonic growth periods. These microtubule

dynamic events could be modulated by MAP1a. This study demonstrates that MAP1a is able to increase growth and stability of microtubules to a limited extent that also allows shortening events.

MAP1a light chain molecules have demonstrated the ability to have a significant impact on microtubule organization. In this study the ability of LC3 to modulate microtubule dynamics was similar to MAP1a. Heavy chain–light chain interactions have shown that MAP1a inhibits the effect of light chain molecules on alter microtubule organization (Villeneuve, 2003). MAP1a may also modulate microtubule dynamics indirectly by regulating the actions of light chain molecules. The importance of MAP1a-light chain interactions is an important area of future research.

REFERENCES

Addison, C.J. 1997. Microtubule Associated 2 (MAP2) expression in transiently transfected P19 embryonal carcinoma cells. M. Sc. Thesis, University of Ottawa, Canada.

Aizawa, H., Emori, Y., Mori, A., Mirofushi, H., Sakai, H. and Suzuki, K. 1991. Functional analysis of the domain structure of microtubule-associated protein 4. *J. Biol. Chem.* **266**: 9841-9846.

Audebert, S., Desbruyeres, E., Gruszczynski, C., Koulakoff, A., Gros, F., Denoulet, P. and Edde, B. 1993. Reversible polyglutamylation of alpha and beta tubulin and microtubule dynamics in mouse brain neurons. *Neuron* **8**: 831-842.

Audebert, S., Koulakoff, A., Berwald-Netter, Y., Gros, F., Denoulet, F. and Edde, B. 1994. Developmental regulation of polyglutamylated alpha and beta tubulin in mouse brain neurons. *J. Cell. Sci.* **107**: 2313-2322.

Avila, J., Dominguez, J. and Diaz-Nido, J. 1994. Regulation of microtubule dynamics by microtubule associated protein expression and phosphorylation during neuronal development. *Int. J. Dev. Biol.* **38**: 13-25.

Baas, P.W. and Black, M.M. 1990. Individual microtubules in the axon consist of domains that differ in both composition and stability. *J. Cell. Biol.* **111**: 495-509.

Banjaree, A., Roach, M.C., Trcka, P., Luduena, R.F. 1990. Increased microtubule assembly in bovine brain tubulin lacking the type III isotype of beta tubulin. *J. Biol. Chem.* **265**: 1794-1799.

Black, M.M., Slaughter, T. and Fischer, I. 1994. MAP1b is concentrated in the distal region of growing axons. *J. Neurosci* **14**: 857-870.

Bloom, G.S., Luca, F. and Vallee, R.B. 1985. MAP1b: identification of a major component of the neuronal cytoskeleton. 1985. *Proc. Natl. Acad. Sci. U.S.A.* **82**: 5404-5408.

Bloom, G.S., Schoenfeld, T.A. and Vallee, R.B. 1984. Widespread distribution of the major polypeptide component of MAP1 in the nervous system. *J. Cell. Biol.* **98**: 320-330.

Bloom, G.S. and Vallee, R.B. 1983. Association of MAP2 with microtubules and intermediate filaments in cultured brain cells. *J. Cell Biol.* **96**: 5123-1532.

Bonnet, C., Boucher, D., Lazereg, S., Pedrotti, B., Islam, K., Denoulet,P., and Larcher, J.C. 2001. Differential binding regulation of microtubule-associated proteins MAP1A, MAP1B, and MAP2 by tubulin polyglutamylation. *J.Biol.Chem.* **276**: 12839-12848.

Boucher, D., Larcher, J.C., Gros, F. and Denoulet, P. 1994. Polyglutamylation of tubulin as a progressive regulator of in vivo interactions between the MAP tau and tubulin. *Biochem.* **33**: 12471-12477.

Brandt, R. and Lee, G. 1993. Functional organization of microtubule-associated protein tau. *J. Biol. Chem.* **268**: 3414-3419.

Brugg, B. and Matus, A. 1991. Phosphorylation determines the binding of MAP2 to microtubules in living cells. *J. Cell Biol.* **114**: 735-743.

Brugg, B., Reddy, D. and Matus, A. 1993. Attenuation of MAP1b expression by antisense oligodeoxynucleotides inhibits initiation of neurite outgrowth. *Neurosci.* **52**: 489-496.

Bulinski, J.C., Richards, J.E. and Pimperno, G. 1988. Posttranslational modifications of alpha tubulin: detyrosination and acetylation differentiate populations of interphase microtubules in cultured cells. *J. Cell Biol.* **106**: 1213-1220

Cassimeris, L. 1993. Regulation of microtubule dynamic Instability. *Cell Mot. Cytoskel.* **26**: 275-281.

Cassimeris, L., Pryer, N.K. and Salmon, E.D. 1988. Real time observations of microtubule dynamic instability in living cells. *J. Cell. Biol.* **107**: 2223-2231.

Chapin, S.J. and Bulinski, J.C. 1992. Microtubule stabilization by assembly promoting microtubule associating proteins: a repeat performance. *Cell Mot. Cytoskel.* **23**: 236-243.

Chapin, S.J., Lue, C.M., Yu, M.T. and Bulinski, J.C. 1995. Differential expression of alternatively spliced forms of MAP4: a repertoire of structurally different microtubule binding domains. *Biochem.* **34**: 2289-2301.

Chen, J., Kanai, Y., Cowan, N.J. and Hirokawa, N. 1992. Projection domains of MAP2 and tau determine spacing between microtubules in dendrites and axons. *Nature* **360**: 674-677.

Choudhary, S., Joshi, K. and Gill, K.D. 2001. Possible role of enhanced microtubule phosphorylation in dichlorvos induced delayed neurotoxicity in rat. *Brain Res.* **897**: 60-70.

Cowan, N.J., Lewis, S.A., Gu, W. and Burgoyne, R.D. 1988. Tubulin isotypes and their interaction with microtubule associated proteins. *Protoplasma* **145**: 106-111.

Crandall, J.E. and Fischer, I. 1989. Developmental regulation of MAP2 expression in regions of mouse brain. *J Neurochem.* **53**: 1910-1917.

Cross, D., Dominguez, J., Maccioni, R.B. and Avila, J. 1991. MAP1 and MAP2 binding sites at the c terminus of beta tubulin. *Biochem.* **30**: 4362-4366.

Dotti, C.G., Banker, G.A. and Binder, L.I. 1987. The expression and distribution of the microtubule-associated protein 2 in hippocampal neurons in the rat *in situ* in cell culture. *Neurosci.* **23**: 121-130.

Drubin, D.G., Feinstein, S.C., Shooter, E.M. and Kirschner, M.W. 1985. Nerve growth factor-induced neurite outgrowth in PC12 cells involves the coordinate induction of microtubule assembly and microtubule assembly promoting factors. *J. Cell Biol.* **101**: 1799-1807.

Drubin, D.G. and Kirschner, M.W. 1986. Tau protein function in living cells. *J. Cell Biol.* **103**: 2739-2746.

Dhamodharan, R. and Wadsworth, P. 1995. Modulation of microtubule dynamic instability in vivo by brain MAPs. *J. Cell Sci.* **108**: 1679-1689.

Evan, G.I., Lewis, G.K., Ramsay, G., and Bishop, J.M. 1985. Isolation of monoclonal antibodies specific for the human c-myc proto-oncogene product. *Mol.Cell Biol.* **5**: 3610-3616.

Falconer, M.M., Echeverri, C.J., and Brown, D.L. 1992. Differential sorting of beta-tubulin isotypes into colchicine-stable microtubules during neuronal and muscle differentiation of embryonal carcinoma cells. *Cell Mot. Cytoskel.* **21**: 313-325.

Falconer, M.M., Vaillant, A.R., Reuhl, K.R., Laferriere, N. and Brown, D.L. 1994. The molecular basis of microtubule stability in neurons. *Neurotoxicol.* **15**: 109-122.

Fawcett, J.W., Matthews, G., Housden, E., Goedert, M. and Matus, A. 1994. Regenerating sciatic nerve axons contain the adult rather than the embryonic pattern of microtubule associated proteins. *Neurosci.* **61**: 789-804.

Fellous, A., Prasad, V., Ohayon, R., jordan, M.A. and Luduena, R.F. 1994. Removal of the projection domain of MAP2 alters its interaction with tubulin. *J. Prot. Chem.* **13**: 381-391.

Ferria, A., Busciglio, J. and Caceres, A. 1989. Microtubule formation and neurite growth in cerebellar macroneurons which develop in vitro: evidence for the involvement of MAP1a, HMW-MAP2 and tau. *Dev. Brain Res.* **49**: 215-228.

Field, D.J., Collins, R.A. and Lee, J.C. 1984. Heterogeneity of vertebrate tubulins. *Proc. Natl. Acad. Sci. U.S.A.* **81**: 4041-4045.

Frappier, T.F., Georgieff, I.S., Brown, K. and Shelanski, M.L. 1994. Tau regualtion of microtubule spacing and bundling. *J. Neurochem.* **63**: 2288-2294.

Fink, J.K., Jones, S.M., Esposito, C., and Wilowski, J. 1996. Human microtubule-associated protein 1A (MAP1A) gene: genomic organization, cDNA sequence, and developmental-and tissue- specific expression. *Genomics* **35**: 577-585.

Fujii, T., Watanabe, M. and Nakemura, A. 1996. Characterization of MAP1a protein kinases from rat brain. *Neurochem. Intl.* **28**: 535-544.

Fujii, T., Watanabe, M., Ogoma, Y., Kondo, Y. and Arai, T. 1993. Microtubule associated proteins MAP1a and MAP1b, interact with F-actin in vitro. *J. Biochem.* **144**: 827-829.

Fukuyama, R., and Rapoport, S.I. 1995. Brain-specific expression of human microtubule-associated protein 1A (MAP1A) gene and it is assignment to human chromosome 15. *J.Neurosci. Res.* **40**: 820-825.

Gamblin, C.T., Nachmanoff, K., Halpain, S. and Willams, R.C. 1996. Recombinant MAP2c reduces the dynamic instability of individual microtubules. *Biochem.* **35**: 12576-12586.

Geodert, M. and Jakes, R. 1990. Expression of separate forms of human tau protein: co-relation with tau pattern in brain and effects on tubulin polymerization. *EMBO J.* **9**: 4225-4230.

Gong, C.X., Wegiel, J., Lidsky, T., Zuck, L., Avila, J., Wisniewski, H.M., Grundke-Iqbal, I. And Iqbal, K. 2000. Regulation of phosphorylation of neuronal microtubule associated proteins MAP1b and MAP2 by protein phosphatase 2A and 2B in rat brain. *Brain Res.* **853**: 299-309.

Gordon-Weeks, P.R. 1993. Organization of microtubules in axonal growth cones: a role for MAP1b. *J. Neurocytol.* **22**: 717-725.

Gurland, G. and Gundersen, G.G. 1995. Stable, detyrosinated microtubules function to localize vimentin intermediate filaments in fibroblasts. *J. Cell Biol.* **131**: 1275-1290.

Gustake, N., Trinczek, B., Biernat, J., Mandelkow, E.-M., and Mandelkow, E. 1994. Domains of τ protein and interactions with microtubules. *Biochemistry* **33**: 9511-9522.

Hammarback, J.A., Obar, R.A., Huges, S.M. and Valee, R.B. 1991. MAP1B is encoded as a polyprotein that is processed to form a complex n-terminal microtubule-binding domain. *Neuron* **7**: 129-139.

Harada, A., Oquchi, K., Okabe, S., Kuno, J., Terada, S., Ohshima, T., Sato-Yoshitake, R., Takei, Y., Noda, T. and Hirokawa, N. 1994. Altered microtubule organization in small calibre axons in mice lacking tau protein. *Nature* **369**: 488-491.

Harrison, A. and Hyams, J.S. 1990. Mapping MAP2. *J. Cell Sci.* **96**: 347-349.

Himmler, A., Dreschel, D., Kischner, M.W. and Martin, D.W. Jr. 1989. Tau consists of a set of proteins with repeated c terminal binding domains and variable n terminal domains. *Mol. Cell Biol.* **91**: 1381-1388.

Ikawa, M., Yamada, S., Nakanishi, T. and Okabe, M. 1999. GFP as a vital marker in mammals. *Curr. Top. Dev. Biol.* **44**: 1-19.

Joshi, H.C. and Cleveland, D.W. 1989. Differential utilization of β-tubulin isotypes in differentiating neurites. *J.Cell Biol.* **109**: 663-673.

Kalcheva, N., Rockwood, J.M., Kress, Y., Steiner, A. and Shafit-Zagardo, B. 1998. Molecular and functional characteristics of MAP-2a: ability of MAP-2a versus MAP-2b to induce stable microtubules in COS cells. *Cell Mot. Cytoskel.* **40**: 272-85.

Kaech, S., Ludin, B. and Matus, A. 1996. Cytoskeletal plasticity in cells expressing neuronal microtubule-associated proteins. *Neuron* **17**: 1189-1199.

Kaech, S., Parmar, H., Roelandse, M., Bornmann and Matus, A. 2001. Cytoskeletal microdifferentiation: a mechanism for organizing morphological plasticity in dendrites. *Proc.Natl. Acad. Sci.*USA. **98**: 7086-7092.

Khan, I.A. and Luduena, R.F. 1996. Phosphorylation of beta III tubulin. *Biochem.* **35**: 3704-3711.

Khawaja, S., Gundersen, G.G. and Bulinski, J.C. 1988. Enhanced stability of microtubules enriched in detyrosinated tubulin is not a direct function of detyrosination level. *J. Cell Biol.* **106**: 141-149.

Kindler, S., Shwanke, B., Schulz, and Garner, C.C. 1990. Complete cDNA sequence encoding rat high and low molecular weight MAP2. *Nucleic Acids Res.* **18**: 2882.

Kreitzer, G., Liao, G., and Gundersen, G.G. 1999. Detyrosination of tubulin regulates the interaction of intermediate filaments with microtubules in vivo via a kinesin-dependent mechanism. *Mol. Biol. Cell* **10**: 1105-1118.

Kuznetsov, S.A., Rodionov, I.V., Nadezhdina, E.S., Murphy, D.B., and Gelfand, V.I. 1986. Identification of a 34-kD polypeptide as a light chain of microtubule-associated protein-1 (MAP-1) and its association with a MAP-1 peptide that binds to microtubules. *J.Cell Biol.* **102**: 1060-1066.

Kuznetsov, S.A., and Gelfand, V.I. 1987. 18 kDa microtubule- associated protein: identification as a new light chain (LC3) of microtubule–associated protein 1 (MAP-1). *FEBS (Fed. Eur. Biochem. Soc.) Lett* **212**:145-148.

Laemmil, U.K. 1970. Cleavage of structural proteins during the assembly of the head of bacteriophage T4. *Nature*. **227**: 680-685.

Laferriere, N.B., MacRae, T., and Brown, D.L. 1997. Tubulin synthesis and assembly in differentiating neurons. *Biochem. Cell Biol.* **75**: 103-117.

Langkopf, A., Hammarback, J.A., Muller, R., Valee, R.B. and Garner, C.C. 1992. Microtubule associated proteins 1a and LC2. *J. Biol. Chem.* **267**: 16561-16566.

Lewis, S.A., Wang, D. and Cowan, N.J. 1988. MAP2 shares a microtubule binding motif with tau protein. *Science* **242**: 936-939.

Lieuvin, A., Labbe, J.C., Doree, M. and Job, D. 1994. Intrinsic microtubule stability in interphase cells. *J. Cell Biol.* **124**: 985-996.

Lopata, M.S. and Cleveland, D.W. 1987. In vivo microtubules are co-polymers of available beta-tubulin isotypes: localization of each of six vertebrate beta tubulin isotypes using polyclonal antibodies elicited by synthetic peptide antigens. *J. Cell Biol.* **105**: 1707-1720.

Littauer, U.Z., Giveon, D., Thierauf, M., Ginzburg, I. And Potingl, H. 1986. Common and distinct tubulin binding sites for MAPs. *Proc. Natl. Acad. Sci. U.S.A.* **83**: 7162-7166.

Lo, M.M.S., Fieles, A.W., Norris, T.E., Dargis, P.G., Caputo, C.B., Scott, C.W., Lee, V. and Goedert, M. 1993. Human tau isoforms confer distinct morphological and functional properties to stably transfected fibroblasts. *Mol. Brain Res.* **20**: 209-220.

Ludueña, R.F. 1993. Are tubulin isotypes functionally significant. *Mol. Biol. Cell.* **4**: 445-457.

Ludueña, R.F. 1998. Multiple forms of tubulin; different gene products and covalent modifications. *Int. Rev. Cytol.* **178**: 207-275.

Ludin, B., Doll, T., Meili, R., Kaech, S. and Matus, A. 1996. Application of novel vectors for GFP tagging of proteins to study microtubule associated proteins. *Gene.* **173**: 107-111.

Ludin, B. and Matus, A. 1998. GFP illuminates the cytoskeleton. *Trends in Cell Biol.* **8**: 72-77.

Mack, T.G.A., Koester, M.P. and Pollerberg, E. 2000. The microtubule-associated protein MAP1b is involved in local stabilization of turning growth cones. *Mol. Cell. Neurosci.* **15**: 51065

MacRae, T.H. 1992. Microtubule organization by cross linking and bundling proteins. *Biochim. Biophys. Acta.* **1160**: 145-155.

Mandelkow, E. and Mandelkow, E.M. 1995. Microtubules and microtubule-associated proteins. *Curr. Opin. Cell Biol.* **7**: 72-81.

Mann, S.S. and Hammarback, J.A. 1994. Molecular characterization of LC3. *J Biol. Chem.* **269**: 11492-11497.

Mann, S.S. and Hammarback, J.A. 1996. Gene localization and developmental expression of LC 3: a common subunit of MAP1a and MAP1b. *J. Neurosci. Res.* **43**: 535-544.

Mei, X., Sweatt, A.J. and Hammarback, J.A. 2000. Regulation of MAP1b subunit composition. *J. Neurosci Res.* **62**: 56-64

Mickey, B. and Howard, J. 1995. Rigidity of microtubules is increased by stabilizing agents. *J. Cell. Biol.* **130**: 909-917.

Mitchison, T. and Kirschner, M. 1984. Dynamic instability of microtubule growth. *Nature* **312**: 237-242.

Müller, R., Kindler, S., and Garner, C.C. 1994. The MAP1 family. In Microtubules, eds. Hyams, J.S., Clive, W.L., pp. 141-154, Wiley-Liss, Inc., NY.

Noble, M., Lewis, S.A., and Cowan, J.N. 1989. The microtubule binding domain of microtubule-associated protein MAP1B contains a repeated sequence motif unrelated to that of MAP2 and tau. *J.Cell Biol.* **109**: 3367-3376.

Noiges, R., Eichinger, R., Kutschera, W., Fischer, I., Nemeth, Z., Wiche, G. and Provost, F. 2002. Microtubule-associated protein 1A (MAP1A) and MAP1B: light chains determine distinct functional properties. *J. Neurosci.* **22**: 2106-2114.

Nixon, R.A. 1998. Dynamic behavior and organization of cytoskeletal proteins in neurons: reconciling old and new findings. *Bioessays* **20**: 798-807.

Oblinger, M.M. and Kost, S.B. 1994. Coordinate regulation of tubulin and microtubule-associated protein genes during development of hamster brain. *Devel. Brain Res.* **77**:45-54.

Olson, K.R., McIntosh, J.R., and Olmsted, J.B. 1995. Analysis of MAP4 function in living cells using green fluorescent protein GFP chimeras. *J.Cell Biol.* **130**: 639-650.

Oudega, M., Touri, F., Deenen, M.G.M., Riederer, B.M. and Marani, E. 1998. Map1a is involved in the early development of the rat spinal cord. *Neurosci. Lett.* **246**: 81-84.

Panda, D., Miller, H.P., Banjaree, A., Luduena, R.F. and Wilson, L. 1994. Microtubule dynamics in vitro are regulated by the tubulin isotype composition. *Proc. Natl. Acad. Sci. U.S.A.* **91**: 11358-11362.

Papasosozmenos, S.C. and Binder, L.I. 1987. Phosphorylation determines two distinct species of tau in the central nervous system. *Cell Mot. Cytoskel.* **8**: 210-226.

Pedrotti, B., Soffientini, A., and Islam, K. 1993. Sulphonate buffers affect the recovery of microtubule-associated proteins MAP1 and MAP2: evidence that MAP1A promotes microtubule assembly. *Cell Mot. Cytoskel.* **25**: 234-242.

Pedrotti, B., Colombo, R. and Islam, K. 1994. MAP1a is an actin binding and cross linking protein. *Cell. Mot. Cytoskel.* **29**: 110-116.

Pedrotti, B. and Islam, K. 1994. Purified native microtubule associated protein MAP1a: kinetics of microtubule assembly and MAP1a/tubulin stoichiometry. *Biochem.* **33**: 12463-12470.

Pedrotti, B. and Islam, K. 1995. MAP1b promotes efficient tubulin polymerization in vitro. *FEBS (Fed. Eur. Biochem. Soc.) Lett.* **371**: 29-31

Pedrotti, B., Ulloa, L., Avila, J., and Islam, K. 1996a. Characterization of microtubule-associated proteins MAP1B: phosphorylation state, light chains, and binding to microtubules. *Biochemistry* **35**: 3016-3023.

Pedrotti, B., Francolini, M., Cotelli, F., and Islam, K. 1996b. Modification of microtubule shape *in vitro* by molecular weight microtubule-associated proteins MAP1A, MAP1B and MAP2. *FEBS (Fed. Eur. Biochem. Soc.) Lett.* **384**:147-150

Pimperno, G., LeDizet, M. and Chang, X. 1987. Microtubules containing acetylated alpha-tubulin in mamallian cells in culture. *J. Cell Biol.* **104**: 289-302.

Pryer, N.K., Walker, R., Skeen, V., Bournas, B.D., Soboeiro, M. and Salmon, E. 1992. Brain MAPs modulate microtubule dynamics in vitro. *J. Cell Sci.* **103**: 965-976.

Ramon-Cuento, A. and Avila, J. 1999. Two modes of MAP1b phosphorylation are differentially regulated during peripheral nerve regeneration. *Brain Res.* **815**: 213-226.

Redecker, V., Rusconi, F., Mary, J., Prome, D. and Rossier, J. 1996. Structure of the c terminal tail of alpha tubulin: increase of heterogeneity from newborn to adult. *J. Neurochem.* **67**: 2104-2114.

Regnard, C., Audebert, S., Desbruyeres, E., Denoulet, P. and Edde, B. 1998. Tubulin polyglutamylase: partial purification and enzymatic properties. *Biochem.* **37**: 8395-8404.

Rusan, N.M., Fagerstrom, C.J., Yvon, A.M., Wadsworth, P., Links, R.M. 2001. Cell cycle-dependent changes in microtubule dynamics in living cells expressing green fluorescent protein-alpha tubulin. *Mol Biol Cell.* **12**: 971-80.

Sattilaro, R.F. 1986. Interaction of MAP2 with actin filaments. *Biochem.* **25**: 2003-2009.

Sato-Yoshitake, R., Shiomura, Y., Miyasaka, H., and Hirokawa, N. 1989. Microtubule-associated protein 1B: molecular structure, localization, and phosphorylation-dependent expression in developing neurons. *Neuron* **3**: 229-238.

Schoenfeld, T.A., McKerracher, L., Obar, R., and Vallee, R.B. 1989. MAP1A and MAP1B are structurally related microtubule-associated proteins with distinct developmental patterns in the CNS. *J. Neurosci.* **9**: 1712-1730.

Schulze, E., Asai, D.J., Bulinski, J.C. and Kirschner, M. 1987. Posttranslational modification and microtubule stability. *J. Cell Biol.* **105**: 2167-2177.

Schulze, E. and Kirschner, M. 1986. Microtubule dynamics in interphase cells. *J. Cell Biol.* **102**:1020-1031.

Shelden, E. and Wadsworth, P. 1993. Observation and quantification of individual microtubule behavior in vivo: microtubule dynamics are cell type specific. *J. Cell Biol.* **120**: 935-945.

Shiomura, Y. and Hirokawa, N. 1987. Colocalization of MAP1a and MAP2 on neuronal microtubules in situ revelaved with double label immunoelectron microscopy. *J. Cell. Biol.* **104**: 1575-1578.

Steffanini, M. DeMartino, C. and Zamboni, L. 1967. Fixation of ejaculated spermatozoa for electron microscopy. *Nature* **216**: 173-174.

Sullivan, K.F. and Cleveland, D.W. 1986. Identification of conserved isotype defining variable region sequences of four vertebrate beta tubulin polypeptide classes. *Proc. Natl. Acad. Sci. U.S.A.* **83**:4327-4331.

Takemura, R., Okabe, S., Umeyama, T., Kanai, Y., Cowan, N.J., and Hirokawa, N. 1992. Increased microtubule stability and alpha tubulin acetylation in cells transfected with microtubule-associated proteins MAP1B, MAP2 and tau. *J. Cell Sci.* **103**: 953-964.

Togel, M., Wiche, G. and Propst, F. 1998. Novel features of the light chain of microtubule associated protein MAP1b: microtubule stabilization, self interaction, actin filament binding, and regulation by heavy chain. *J. Cell Biol.* **143**: 695-707.

Towbin, H., Staehlin, T. and Gordon, J. 1979. Electrophoretic transfer of proteins from polyacrylamide gels to nitrocellulose sheets: procedure and some applications. *Proc. Natl. Acad. Sci. U.S.A.* **76**: 4350-4354.

Trinczek, B., Biernat, J., Baumann, K., Mandelkow, E.M. and Mandelkow, E. 1995. Domains of tau protein, differential phosphorylation and dynamic instability of microtubules. *Mol. Biol. Cell* **6**: 1887-1902.

Tucker, R.P., Binder, L.I. and Mauts, A.I. 1988. Neuronal microtubule-associated proteins in the embryonic avian spinal cord. *J. Comp. Neurol.* **271**: 44-55.

Umeyama, T., Okabe, S., Kanai, Y. and Hirokawa, N. 1993. Dynamics of microtubules bundled by MAP2c. *J. Cell Biol.* **120**: 451-465.

Ungureanu, H. N. 2002. The light chain of MAP1a binds to and stabilizes microtubules. M. Sc. Thesis, University of Ottawa, Canada.

Vaillant, A., Muller, R., Langkopf, A. and Brown, D.L. 1998. Characterization of the microtubule binding domain of MAP1a and its effects on microtubule dynamics. *J. Biol. Chem.* **273**: 13973-13981.

Vallee, R.B., and S.E., Davis. 1983. Low molecular weight microtubule-associated proteins are light chains of microtubule-associated protein 1(MAP 1). *Proc. Natl. Acad. Sci. USA.* **80**: 1342-1346.

Verde, F., Labbe, J.C., Dorree, M. and Karsenti, E. 1990. Regulation of microtubule dynamics by cdc2 protein kinase in cell free extracts of Xenopus eggs. *Nature* **343**: 233-238.

Villasante, A., Wang, D., Dobner, P., Lewis, S.A. and Cowan, N. J. 1986. Six mouse alpha tubulin mRNAs encode five distinct isotypes. *Mol. Cell Biol.* **6**:2409-2419.

Villeneuve, T. 2003. Microtuble associated protein 1A: heavy and light chain interactions. M. Sc. Thesis, University of Ottawa, Canada.

Wandosell, F., Serrano, L., Hernandez, M.A. and Avila, J. 1986. Phosphorylation of tubulin by a calmodulin-dependant protein kinase. *J. Biol. Chem.* **261**: 10332-10339.

Weisshaar, B., Doll, T., and A.Matus. 1992. Reorganization of the microtubular cytoskeleton by embryonic microtubule-associated protein 2 (MAP2c). *Development* **116**: 1151-1161.

Weisshar, B. and Matus, A. 1993. MAP2 and the organization of cellular microtubules. *J Neurocytol.* **22**: 727-734.

White, J. and Stelzer, E. 1999. Photobleaching GFP reveals protein dynamics inside living cells. *Trends Cell Biol.* **9**: 61-65.

Wille, H., Mandelkow, E.M. and Mandelkow, E. 1992. The juvenile microtubule associated protein MAP2c is a rod like molecule that forms antiparallel dimers. *J. Biol. Chem.* **267**: 10737-10742.

Xiang, H. and T.H. MacRae. 1995. Production and utilization of detyrosinated tubulin in developing *Artemia larvae*: Evidence for a tubulin-reactive carboxypeptidase. *Biochem. Cell Biol.* **71**: 673-685.